nature genetics

Article

https://doi.org/10.1038/s41588-025-02429-2

Natural variation in *OsTPS8* confers differential regulation of chalkiness and seed vigor in *indica* and *japonica* rice

Received: 8 May 2024

Accepted: 23 October 2025

Published online: 15 December 2025

Check for updates

Xiaoli Chen[1,4], Yulong Ren[2,4], Hui Dong[1,4], Xiaokang Jiang[1,4], Xiaoming Zheng[2], Erchao Duan[1], Xuan Teng[1], Yunlong Wang[1], Chuanwei Gu[1], Rongbo Chen[1], Qingkai Wang[1], Yongfei Wang[1], Yipeng Zhang[1], Rushuang Zhang[1], Yunpeng Zhang[1], Wenjie Zhao[1], Yu Zhang[1], Xue Yang[1], Lei Zhou[1], Chao Li[1], Tiaofeng Shan[1], Yiqun Bao[3], Yunlu Tian[1], Xi Liu[1], Shijia Liu[1], Tao Guo[1], Mingjiang Chen[1], Haiyang Wang[2] ✉, Yihua Wang[1,4] ✉ & Jianmin Wan[1,2] ✉

Chalkiness and seed vigor are major agronomic traits affecting rice grain quality and productivity, respectively. Little is known about the intrinsic relationship and the regulatory mechanisms of these two traits. Here we identified a chalkiness locus *qPGWC-8*, which encodes trehalose-6-phosphate synthase 8 (OsTPS8) that suppresses trehalose-6-phosphate (Tre6P) biosynthesis by interacting with and inhibiting OsTPS1. A natural promoter variation in *OsTPS8* confers differential transcriptional regulation by OsbHLH001. Elevated expression of *OsTPS8* reduces Tre6P levels and activates the expression of *OsMYBS1* and α-amylase genes, thus promoting starch degradation, chalkiness formation and seed vigor elevation. Two major haplotypes, $OsTPS8^{ASO}$ and $OsTPS8^{IR24}$, were defined by this functional promoter variation, with $OsTPS8^{IR24}$ preferentially selected during the domestication of *indica* rice. Collectively, our findings establish an OsbHLH001-OsTPS8-Tre6P-α-amylase signaling cascade that has a dual role in regulating grain chalkiness and seed vigor, which reveals a molecular link between the appearance quality and seed vigor of rice.

Asian cultivated rice (*Oryza sativa* L.) is a major staple food for half of the world's population[1]. During domestication, Asian cultivated rice has evolved two major subspecies, *indica* and *japonica*, which possess distinct morphological and physiological differentiation and adapt to different ecological conditions[2]. These differences include plant architecture[3], diurnal floret opening time[4], grain quality[5] and nitrogen use efficiency[6]. However, the potential molecular mechanisms underlying the differentiation between *indica* and *japonica* rice have not yet been well studied.

Chalkiness is a major determinant of grain quality and constitutes a complex quantitative trait controlled by several genetic and environmental factors[7]. Environmental factors encompass conditions such as high temperature, shade, drought and nitrogen application during the grain filling stage[8–11]. Additionally, genes involved in grain filling, seed development, synthesis of storage substances and cellular homeostasis, are considered crucial genetic factors affecting chalkiness formation[7]. To date, only two major quantitative trait loci (QTLs), *Chalk5* and

[1]State Key Laboratory of Crop Genetics & Germplasm Enhancement and Utilization, Zhongshan Biological Breeding Laboratory, Jiangsu Nanjing Rice Germplasm Resources National Field Observation and Research Station, Nanjing Agricultural University, Nanjing, China. [2]State Key Laboratory of Crop Gene Resources and Breeding, National Key Facility for Crop Gene Resources and Genetic Improvement, Institute of Crop Sciences, Chinese Academy of Agricultural Sciences, Beijing, China. [3]College of Life Sciences, Nanjing Agricultural University, Nanjing, China. [4]These authors contributed equally: Xiaoli Chen, Yulong Ren, Hui Dong, Xiaokang Jiang, Yihua Wang. ✉e-mail: wanghaiyang@caas.cn; yihuawang@njau.edu.cn; wanjm@njau.edu.cn

https://doi.org/10.1038/s41588-025-02429-2

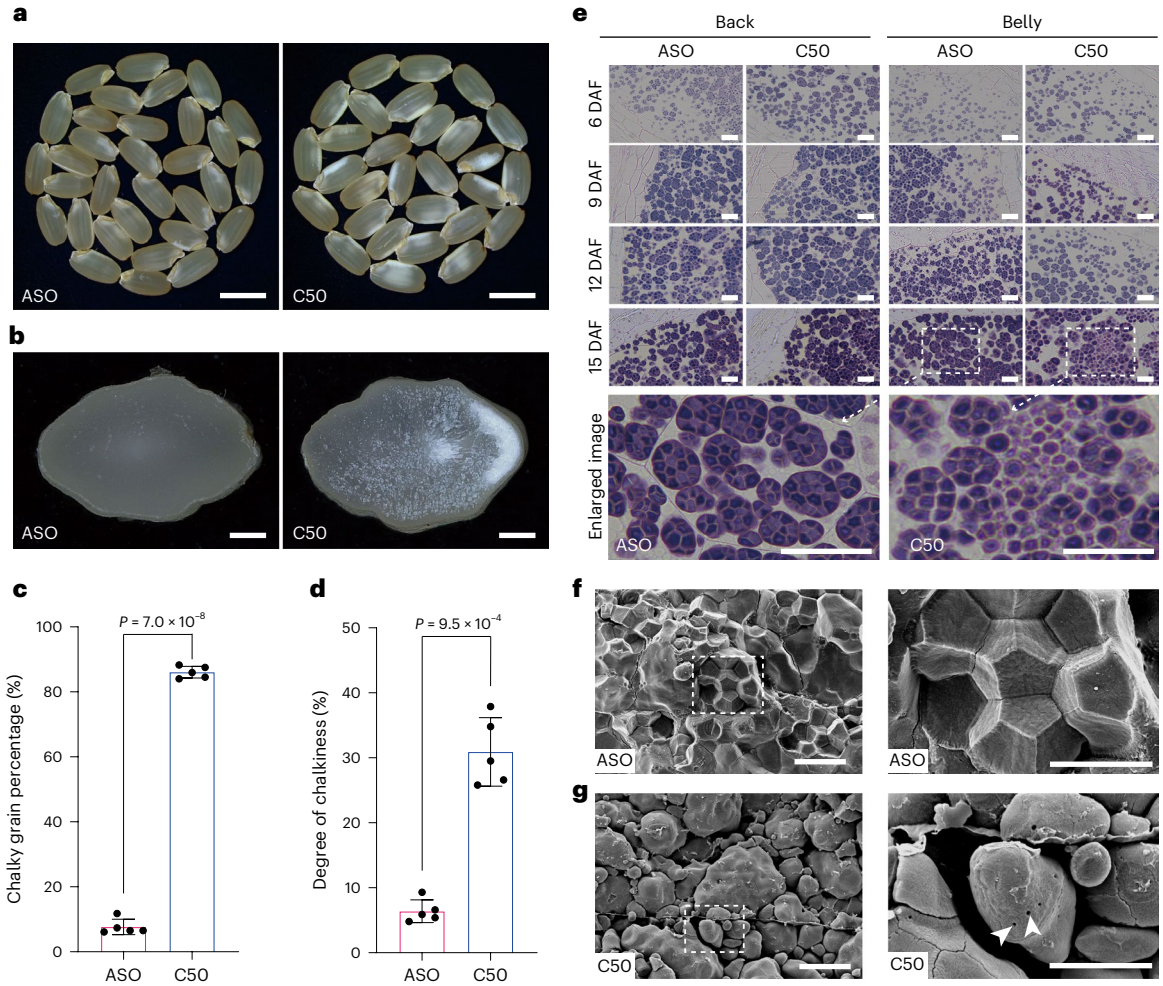

Fig. 1 | Phenotypic characterization of the C50 grains. a, Observations of the mature grains of ASO and C50. **b**, Transverse sections of ASO and C50 mature grains. **c**,**d**, Chalky grain percentage (**c**) and degree of chalkiness (**d**) of ASO and C50 mature grains in 2020 at Nanjing ($n = 5$ plants). **e**, Observations on semi-thin sections of grain back and belly at different developmental stages of ASO and C50. Bottom: enlarged images of the boxed areas in the top sections. **f**,**g**, SEM observations of cross-sections of ASO (**f**) and C50 (**g**) mature grains. Right: enlarged images of the boxed areas on the left. The white arrowheads indicate the holes on the SGs. Values in **c** and **d** are presented as the mean ± s.d. Statistical significance was determined using a two-tailed, paired Student's *t*-test (**c**,**d**). Scale bars, 5 mm (**a**), 0.5 mm (**b**), 20 μm (**e**), 10 μm (**f**,**g**).

WCR1, underlying grain chalkiness with natural variations, have been characterized in rice[12,13]. Recently, a genome-wide association study (GWAS) identified *OsbZIP60*, which affects chalkiness formation by regulating the unfolded protein response (UPR)[14]. Notably, these three high chalkiness alleles are all from *indica* varieties, which is consistent with the notion that chalkiness levels in *indica* are notably higher than those in *japonica*[15,16]. However, little is known regarding the molecular mechanism underlying the divergence of chalkiness formation between *indica* and *japonica* subspecies.

Seed vigor, as an important trait in crop production, determines the potential for seed germination, seedling growth and stress tolerance[17]. High-vigor seeds possess the ability to germinate and establish seedlings rapidly and uniformly in the field, thereby enhancing weed competitiveness and reducing yield losses[18]. Previous studies identified many QTLs and genes affecting seed vigor[19–21]. Generally, *indica* rice displays higher seed vigor than *japonica* rice[22,23]. However, the genetic regulatory mechanism underlying the differential seed vigor between *indica* and *japonica* subspecies remains essentially unexplored. Moreover, the intrinsic relationship and connection between grain chalkiness and seed vigor have not been exploited.

In this study, we report the isolation of a grain chalkiness locus *qPGWC-8* using a map-based cloning approach with a genetic population derived from the *indica* variety IR24 and *japonica* variety Asominori (ASO). We show that *qPGWC-8* encodes trehalose-6-phosphate synthase 8 (OsTPS8), which positively regulates both grain chalkiness and seed vigor in rice. OsTPS8 inhibits OsTPS1 activity and negatively regulates the production of trehalose-6-phosphate (Tre6P), which functions as a signal to inhibit α-amylase activity. Furthermore, *OsTPS8* has two haplotypes, $OsTPS8^{ASO}$ and $OsTPS8^{IR24}$. Natural variation in the *OsTPS8* promoter affects the binding ability of the transcription activator OsbHLH001. In addition, $OsTPS8^{IR24}$ has undergone intensive selection during the domestication of *indica* rice in low latitudes because of its higher seed vigor. Our findings unveil an important role of *OsTPS8* in Tre6P biosynthesis contributing to both grain chalkiness and seed vigor, and provides valuable targets for genetic improvement in rice.

Results

Chalkiness phenotype identification of CSSL50

We previously reported that CSSL50 (C50), derived from the chromosome segmental substitution lines (CSSLs) constructed by insertion of IR24 (an *indica* variety with high chalkiness) segments into ASO (a *japonica* variety with low chalkiness) background[24], stably displayed high grain chalkiness and exhibited a white belly compared with the ASO in Nanjing (119° E, 32° N) and Hainan (110° E, 18° N) (Fig. 1a–d and Supplementary Table 1). There were no significant differences in other

https://doi.org/10.1038/s41588-025-02429-2

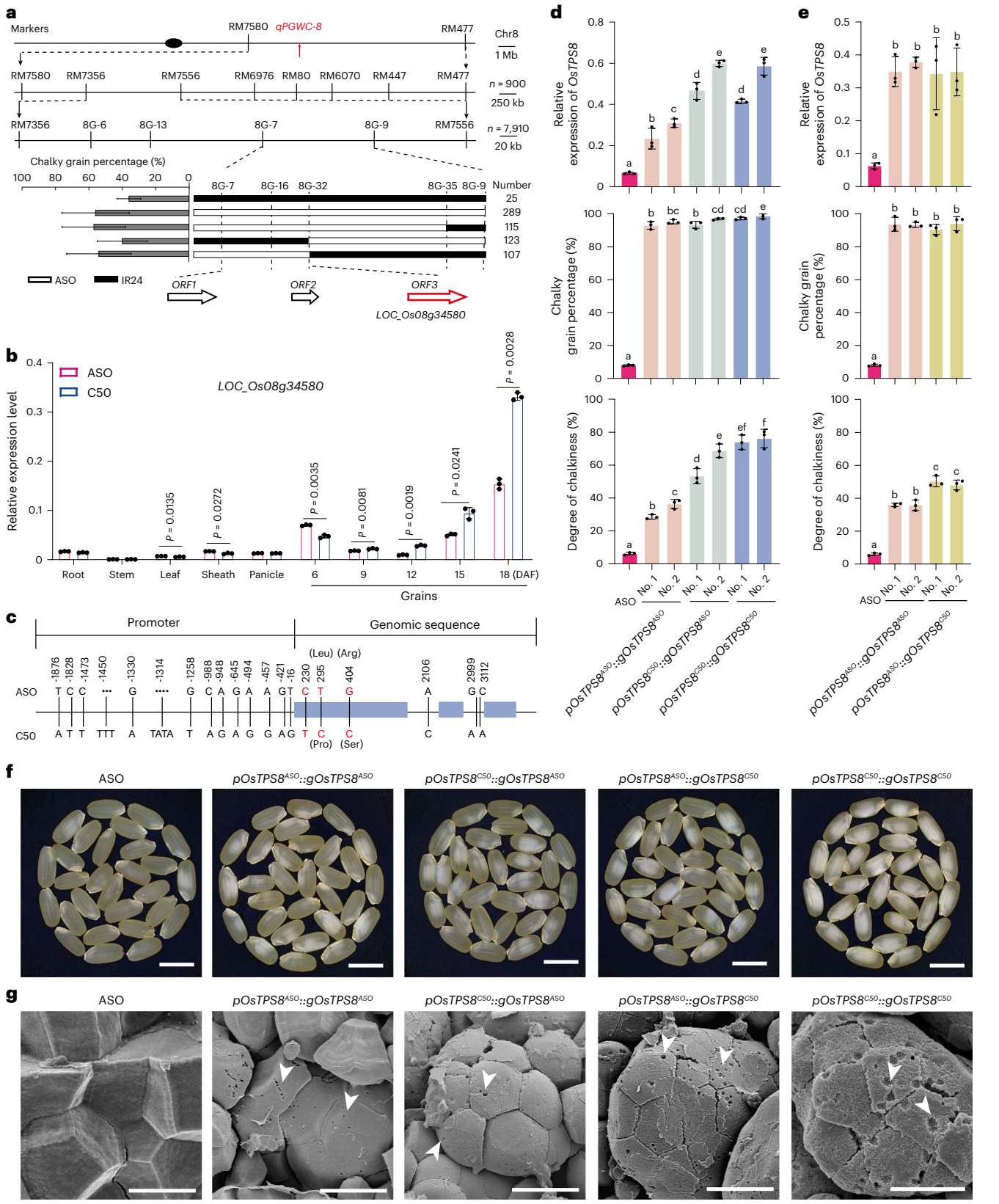

Fig. 2 | Map-based cloning and transgenic verification of *qPGWC-8*. **a**, Fine-mapping of the *qPGWC-8* locus. The *qPGWC-8* locus was firstly mapped between the molecular markers 8G-7 and 8G-9 on chromosome 8 (ref. 24); then, it was finely located to a 35-kb region between markers 8G-7 and 8G-32. **b**, Comparative expression pattern of *OsTPS8* in ASO and C50 ($n = 3$ plants). **c**, Nucleotide sequence polymorphisms of *OsTPS8* between ASO and C50. The SNPs marked in red are located in the exon region, resulting in two amino acid substitutions. **d**,**e**, *OsTPS8* expression level, chalky grain percentage and degree of chalkiness of *OsTPS8* transformants. The genomic sequences of *OsTPS8* from ASO or C50 were driven by either the ASO or C50 promoter (**d**). The genomic sequences of *OsTPS8* from ASO or C50 were driven by ASO promoter (**e**) ($n = 3$ plants). **f**,**g**, Mature grain appearance (**f**) and SEM images (**g**) of the *OsTPS8* transgenic lines. The white arrowheads indicate the holes on the SGs. Values are presented as the mean ± s.d (**b**,**d**,**e**). Statistical significance was determined using a two-tailed, paired Student's *t*-test (**b**). The different lowercase letters indicate significant differences ($P < 0.05$) based on a one-way ANOVA with Dunnett's multiple comparisons test (**d**,**e**). Scale bars, 5 mm (**f**), 5 μm (**g**).

https://doi.org/10.1038/s41588-025-02429-2

major agronomic traits and storage substance accumulation between ASO and C50 (Supplementary Fig. 1).

To determine the cause of chalkiness, we examined the ultrastructure of grains at different developmental stages. At 15 days after flowering (DAF), starch grains in the belly of ASO grains developed typical turtle shell structures, while irregular starch grains with internal granules clearly separated from each other were readily observed in C50; many starch granules (SGs) were lightly stained, suggesting a compromised starch accumulation in C50 (Fig. 1e). Scanning electron microscopy (SEM) observations showed that SGs in the mature endosperm were densely and regularly arranged in ASO grains, whereas in the opaque part of C50 grains, loosely packed, irregularly scattered spherical SGs with large spaces were observed. In addition, the abnormal SGs of C50 exhibited many holes on the surface (Fig. 1f,g), which differed significantly from previously reported chalky or even floury grains[25]. Nevertheless, starch-synthesis-related enzymes showed similar accumulation patterns at both the mRNA and protein levels during grain filling stages between ASO and C50 (Supplementary Fig. 2). These results indicate that the chalkiness of C50 originates from abnormal SGs.

Map-based cloning of *qPGWC-8*

Previously, the *qPGWC-8* locus was mapped to a 142-kb physical region between the molecular markers 8G-7 and 8G-9 on chromosome 8 (ref. 24). To fine-map *qPGWC-8*, we narrowed down the interval to a 35-kb region between the markers 8G-7 and 8G-32, which harbors three putative open reading frames (ORFs) (Fig. 2a). The Plant Public RNA-Seq Database predicted that *ORF1* was barely expressed in all tissues tested. *ORF2* and *ORF3* were both constitutively expressed. *ORF3* was highly expressed in grains and had higher expression in C50 than in ASO from 9 DAF during grain filling (Fig. 2b and Supplementary Fig. 3). Therefore, we suspected that *ORF3* (*LOC_Os08g34580*) most probably represents the candidate gene for *qPGWC-8*. *LOC_Os08g34580* encodes a member of the trehalose-6-phosphate synthase family (OsTPS8). There are multiple differences in the promoter region of *OsTPS8* and three single-nucleotide polymorphisms (SNPs) in the coding regions, the latter two SNPs resulting in two amino acid substitutions in the OsTPS8 protein between ASO and C50 (Fig. 2c).

To confirm whether *OsTPS8* controls chalkiness formation, we transformed the genomic region of *OsTPS8* derived from ASO (*gOsTPS8*^{ASO}) or C50 (*gOsTPS8*^{C50}) driven by their respective native promoter (*pOsTPS8*^{ASO} or *pOsTPS8*^{C50}) into ASO. All transgenic lines with elevated expression of *OsTPS8* exhibited high grain chalkiness (Fig. 2d,e). Among them, the *pOsTPS8*^{C50}*::gOsTPS8*^{ASO} lines exhibited higher *OsTPS8* expression levels and higher chalkiness than the *pOsTPS8*^{ASO}*::gOsTPS8*^{ASO} lines, suggesting that variations in the *OsTPS8* promoter region in C50 contribute to its elevated chalkiness (Fig. 2d). Furthermore, despite the comparable expression levels of *OsTPS8*, the chalkiness of the *pOsTPS8*^{ASO}*::gOsTPS8*^{C50} lines was significantly higher than that of the *pOsTPS8*^{ASO}*::gOsTPS8*^{ASO} lines, suggesting that the two amino acid substitutions of OsTPS8 in C50 may also contribute to its increased chalkiness (Fig. 2e). Notably, small holes were readily observed on abnormal SGs in mature grains of all transgenic lines (Fig. 2f,g). These results verify that *OsTPS8* is the gene responsible for *qPGWC-8*.

OsTPS8 negatively regulates Tre6P synthesis through interacting with OsTPS1

Trehalose-6-phosphate synthase (TPS) catalyzes the synthesis of Tre6P from UDP-glucose and glucose-6-phosphate. Phylogenetic analysis showed that OsTPSs can be divided into two classes. OsTPS8 belongs to the class II TPS family and shares the highest homology with OsTPS5 and OsTPS9 (Supplementary Fig. 4). Observation of the protoplasts of the *pOsTPS8::OsTPS8*-green fluorescent protein (*GFP*) transgenic seedlings showed that OsTPS8^{ASO}-GFP and OsTPS8^{C50}-GFP were localized in the cytosol (Fig. 3a and Supplementary Fig. 5). Further differential centrifugation with the *pOsTPS8::OsTPS8-GFP* developing grains confirmed the cytosolic localization of OsTPS8-GFP (Fig. 3b). Previous studies showed that only class I clade possesses TPS catalytic activity and that OsTPS1 may form complexes with class II TPSs to potentially modify Tre6P levels[26,27]. To test whether OsTPS8 possesses TPS activity, we transformed *OsTPS8*^{ASO} or *OsTPS8*^{C50} into the yeast *tps1* and *tps2* mutants. Neither *OsTPS8*^{ASO} nor *OsTPS8*^{C50} could rescue the glucose growth defects of the yeast *tps1* mutant or the heat-sensitivity of the yeast *tps2* mutant[26] (Supplementary Fig. 6a). Consistently, in vitro activity assays showed that OsTPS8 did not generate detectable levels of Tre6P, suggesting that OsTPS8 lacks typical TPS activity (Supplementary Fig. 6b).

To investigate whether OsTPS8 regulates OsTPS1 activity, we performed yeast two-hybrid (Y2H) and luciferase complementary imaging (LCI) assays, confirming the interaction between OsTPS8 and OsTPS1. Notably, OsTPS8^{C50} exhibited stronger interactions with OsTPS1 than OsTPS8^{ASO} (Fig. 3c,d). We further validated this interaction using a co-immunoprecipitation (co-IP) assay (Fig. 3e). Thus, we hypothesized that this interaction regulates OsTPS1 activity. To confirm this notion, we initially expressed OsTPS1 in *Escherichia coli* but failed, possibly because of its toxicity. Then, we transformed *p35S::OsTPS1-GFP* into protoplasts from the *OsTPS8* knockout (KO) plants and immunoprecipitated the OsTPS1-containing protein complexes to determine its enzymatic activity in vitro (Supplementary Fig. 7). Intriguingly, Tre6P synthesis was gradually compromised with increasing amounts of GST-OsTPS8, suggesting that OsTPS8 inhibits the enzymatic activity of OsTPS1 complexes. Moreover, the inhibitory effect of OsTPS8^{C50} was significantly stronger than that of OsTPS8^{ASO} (Fig. 3f).

Furthermore, we found that the Tre6P contents in C50 grains at different developmental stages were uniformly lower than those of ASO grains (Supplementary Fig. 8). Moreover, the Tre6P contents in mature grains of the above *OsTPS8* transgenic lines were all decreased significantly, compared to the wild-type (WT) control (Fig. 3g), suggesting that Tre6P could suppress chalkiness formation in rice grains. To verify this notion, we downregulated the expression of *OsTPS1* via RNA interference (RNAi) using an endosperm-specific promoter (*pGluC*). These RNAi lines possessed decreased Tre6P content, increased chalkiness and abnormal SGs resembling those of the C50 grains (Fig. 3h–k and Extended Data Fig. 1). Collectively, these results indicate that OsTPS8 negatively regulates Tre6P biosynthesis, leading to elevated grain chalkiness.

Fig. 3 | OsTPS8 interacts with OsTPS1 to inhibit Tre6P synthesis. a, Subcellular localization of OsTPS8-GFP in rice protoplasts from the *pOsTPS8::OsTPS8-GFP* transgenic lines. Scale bar, 10 μm. **b**, Subcellular fractionation and immunoblotting of OsTPS8 in the developing grains of the *pOsTPS8::OsTPS8-GFP* lines. T indicates the total protein extract. S2 and P2 are the supernatant and pellet obtained after centrifugation at 2,000*g*; S13 and P13 are the supernatant and pellet obtained after centrifugation at 13,000*g*; S100 and P100 are the supernatant and pellet obtained after centrifugation at 100,000*g*. Anti-cFBPase and anti-H3 antibodies were used as cytoplasmic and nuclear markers, respectively. **c**, OsTPS8 interacts with OsTPS1 in the Y2H assay. BD, binding domain; AD, activation domain. **d**, LCI assay showing the interactions between OsTPS1 and OsTPS8. **e**, Co-IP assay showing that OsTPS8-GFP but not free GFP could be precipitated by OsTPS1-FLAG. **f**, The effect of OsTPS8 on the enzymatic activity of OsTPS1 complexes ($n = 3$ biological replicates). **g**, The contents of Tre6P in the mature grains of the ASO, C50 and OsTPS8 transgenic lines ($n = 3$ plants). FW, fresh weight. **h**–**k**, Expression levels of *OsTPS1* (**h**), Tre6P content (**i**), chalky grain percentage (**j**) and degree of chalkiness (**k**) in the *pGluC::RNAi-OsTPS1* lines in the ASO background ($n = 3$ plants). Values are presented as the mean ± s.d (**f**,**g**). Statistical significance was determined using a two-tailed, paired Student's *t*-test (**g**–**k**). The different lowercase letters indicate significant differences ($P < 0.05$) based on a one-way ANOVA with Dunnet's multiple comparisons test (**f**). The subcellular fractionation and immunoblotting, Y2H, LCI and co-IP assays were done independently three times with similar results.

https://doi.org/10.1038/s41588-025-02429-2

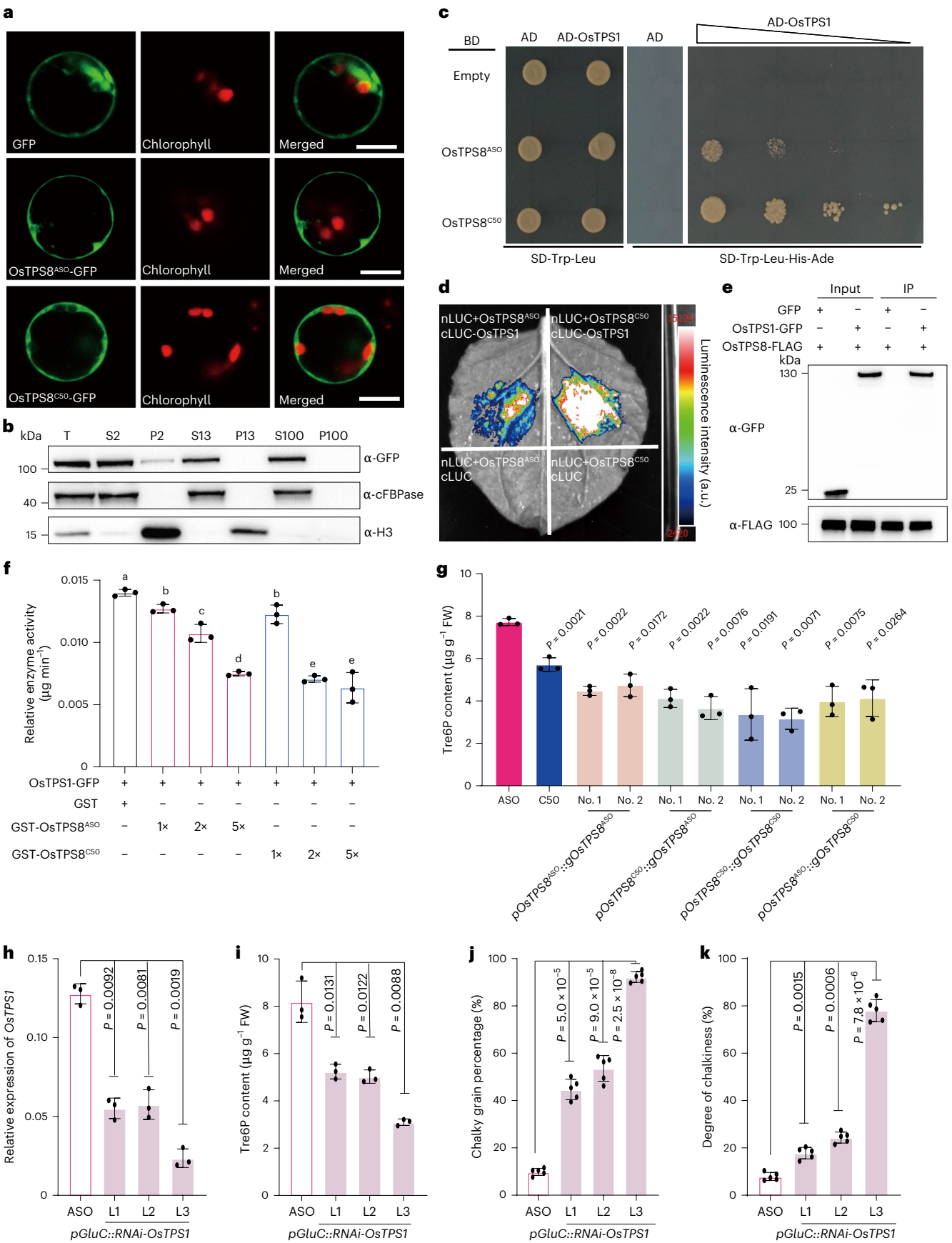

https://doi.org/10.1038/s41588-025-02429-2

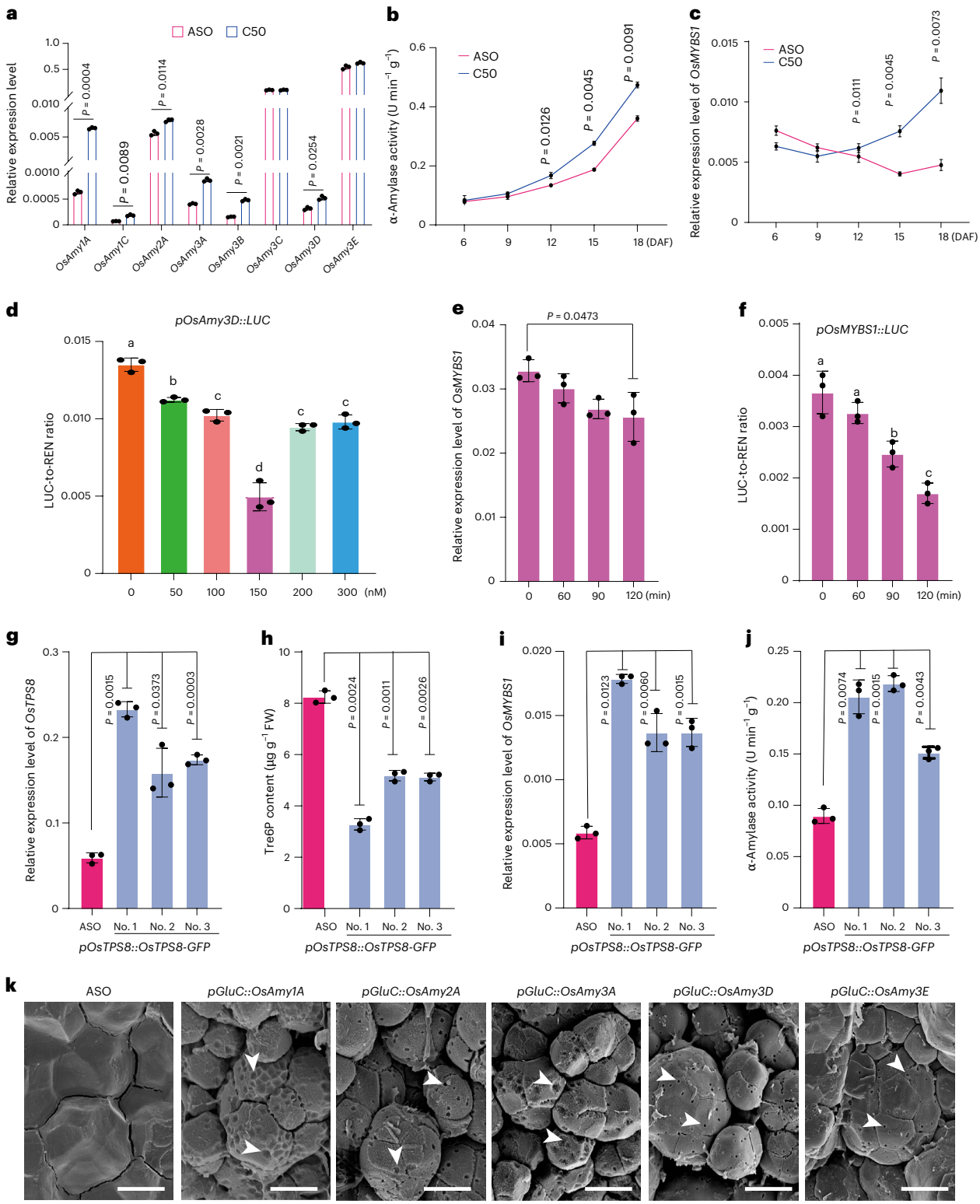

Fig. 4 | Higher α-amylase activity leads to elevated starch degradation. **a**, Expression levels of α-amylase genes in ASO and C50 grains at 15 DAF ($n = 3$ plants). **b**, The α-amylase activities of grains at different developmental stages ($n = 3$ plants). **c**, Expression level of *OsMYBS1* in the ASO and C50 grains at different developmental stages ($n = 3$ plants). **d**, Transactivation of the *OsAmy3D* promoter by Tre6P treatment in rice protoplasts; 0–300 nM Tre6P treatments for 120 min were used in this assay ($n = 3$ biological replicates). **e**, Analysis of the expression level of endogenous *OsMYBS1* in rice protoplasts after 150 nM Tre6P treatment for 0–120 min ($n = 3$ biological replicates). **f**, Transcription inhibition of the *OsMYBS1* promoter by 150 nM Tre6P treatment for 0–120 min in rice protoplasts using the reporter plasmids *pOsMYBS1::LUC* ($n = 3$ biological replicates). **g**–**j**, *OsTPS8* expression level (**g**), Tre6P content (**h**), *OsMYBS1* expression level (**i**) and α-amylase activity (**j**) in the *pOsTPS8::OsTPS8-GFP* transgenic plants ($n = 3$ plants). **k**, SEM observations of mature grains of α-amylase gene overexpression lines. The white arrowheads indicate the holes on the SGs. Scale bar, 10 μm. Values are presented as the mean ± s.d (**a**–**j**). Statistical significance was determined using a two-tailed, paired Student's *t*-test (**a**–**c**,**e**,**g**–**j**). The different lowercase letters indicate significant differences ($P < 0.05$) based on a one-way ANOVA with Dunnet's multiple comparisons test (**d**,**f**).

Tre6P affects the transcription of α-amylase genes, resulting in altered starch degradation

Previous studies reported that the pin holes on the surface of SGs in chalky grain are caused by abnormal starch degradation mediated by the overexpression of α-amylase genes[28], and that lower Tre6P acts as a signal for energy mobilization in seed germination, leading to enhanced transcription of α-amylase genes, a process positively regulated by *OsMYBS1* (ref. 29). Thus, we postulated that the higher chalkiness phenotype of C50 might be underpinned by lower Tre6P levels, and higher expression levels of *OsMYBS1* and α-amylase genes. Consistent with this notion, quantitative PCR with reverse transcription (RT–qPCR) and immunoblot analyses revealed higher expression levels of α-amylase genes and *OsMYBS1*, and higher α-amylase protein abundances and activities in C50 compared to ASO during grain development (Fig. 4a–c and Supplementary Fig. 9). To further test whether Tre6P affects the transcription of α-amylase genes through *OsMYBS1*, we conducted a transient expression experiment using rice protoplasts transformed with an amylase 3D promoter-driven *LUC* gene (*pOsAmy3D::LUC*) followed by treatment with several concentrations of Tre6P. When *pOsAmy3D::LUC* was transformed alone, Tre6P treatment reduced the LUC-to-*Renilla* (REN) LUC ratio, which was intensified with increasing Tre6P concentration (Fig. 4d). These observations suggest that Tre6P downregulates the expression of α-amylase genes in rice grains. In addition, endogenous *OsMYBS1* transcripts in rice protoplasts were significantly downregulated when supplemented with 150 nM Tre6P (Fig. 4e). Moreover, Tre6P treatment significantly diminished the LUC activity of the *OsMYBS1* promoter in protoplasts transformed with *pOsMYBS1::LUC* (Fig. 4f). Together, these results suggest that Tre6P inhibits the expression of *OsMYBS1* and α-amylase genes. Furthermore, we observed decreased expression of α-amylase genes in 12 DAF grains of the *OsMYBS1* KO mutants and increased expression of *OsMYBS1* and α-amylase activity in the *pOsTPS8::OsTPS8-GFP* transgenic lines with reduced Tre6P content (Fig. 4g–j and Extended Data Fig. 2).

To further substantiate the association between abnormal starch degradation and chalkiness, we specifically overexpressed α-amylase genes, including *Amy1A*, *Amy2A*, *Amy3A*, *Amy3D* and *Amy3E*, driven by *pGluC*. Remarkably, the grains of positive transgenic lines of all five genes exhibited a chalky or even floury appearance (Extended Data Fig. 3). Interestingly, SEM observations revealed that these lines developed irregular SGs with many holes and pits on the surface, which was more severe than C50 (Fig. 4k). Taken together, these results suggest that the chalkiness phenotype in C50 is caused by reduced Tre6P content and increased starch degradation at the late stages of grain development.

OsbHLH001 differentially regulates *OsTPS8* transcription

To determine functional variations of *OsTPS8* contributing to chalkiness, we analyzed the genome variations of this gene with 331 Asian cultivated rice accessions (Supplementary Table 3). Single-gene association analysis shows that three tightly linked SNPs (-421, -645 and -948 bp, where the hyphen indicates the distance upstream from the start codon of *OsTPS8*) in the promoter region were highly associated with grain chalkiness (Fig. 5a). Based on the three SNPs, these rice accessions could be classified into two haplotypes: $OsTPS8^{ASO}$ (with the A/G/G variations associated with lower chalkiness) and $OsTPS8^{IR24}$ (with the G/A/A variations associated with higher chalkiness) (Fig. 5b and Supplementary Fig. 10). Consistently, we found that the expression level of *OsTPS8* was significantly lower in 16 accessions with $OsTPS8^{ASO}$ than 18 accessions with $OsTPS8^{IR24}$ (Fig. 5c).

To further identify the functional variations of *OsTPS8*, we compared the putative transcription factor binding sites in promoters using PlantPAN 4.0 (http://plantpan.itps.ncku.edu.tw). Analysis of the *OsTPS8* promoter region revealed the presence of many hormone-responsive elements (abscisic acid, auxin and methyl jasmonate) and light-responsive elements (Supplementary Table 4). Strikingly, we found that the functional SNP (A/G) at -645 bp in the $OsTPS8^{C50}$ promoter region resulted in an additional CANNTG motif, typically recognized by bHLH-type transcription factors. Notably, *OsbHLH001* was predominantly expressed in developing grains with increasing transcript levels during seed development[30], thus it was selected as a candidate upstream regulator of *OsTPS8* (Extended Data Fig. 4a). Consequently, a yeast one-hybrid (Y1H) experiment was performed to show that OsbHLH001 could indeed bind to the $pOsTPS8^{C50}$ promoter (Fig. 5d). Furthermore, an electrophoretic mobility shift assay (EMSA) revealed that OsbHLH001 could bind to the CAAGTG motif (Fig. 5e). Consistently, transient expression assays in rice protoplasts showed that OsbHLH001 could activate the expression of $pOsTPS8^{C50}$ and $pTPS8^{ASO}G\text{-}A$ (a site-directed mutation from G to A in the background of ASO), but not $pOsTPS8^{ASO}$ (Fig. 5f). Moreover, endosperm-specific overexpression of *OsbHLH001* in C50 significantly elevated the expression level of *OsTPS8* and ultimately led to even higher grain chalkiness compared to C50 (Fig. 5g,h and Extended Data Fig. 4b–e).

To further validate the effect of SNP (−645 A/G) on chalkiness, we performed a targeted base-editing mutation at this site in ASO (Fig. 5i). Seven positive gene-edited (PGE) plants were obtained with an average editing efficiency of 2% (Extended Data Fig. 4f,g). Compared with ASO, the expression levels of *OsTPS8* in the grains of the PGE lines were significantly upregulated, accompanied by increased grain chalkiness (Fig. 5j). In summary, the −645 A/G SNP represents a major natural variation in the *OsTPS8* promoter that affects the binding of OsbHLH001 and the expression level of *OsTPS8*, consequently affecting the level of grain chalkiness.

$OsTPS8^{IR24}$ is artificially selected during *indica* rice domestication

To determine whether *OsTPS8* underwent selection during rice domestication, we investigated the proportions of two *OsTPS8* haplotypes using wild rice (*Oryza rufipogon* and *Oryza nivara*), landraces and Chinese cultivars[31]. Our result revealed that $OsTPS8^{IR24}$ preexists in wild rice at ~11%; its proportion increased dramatically in *indica* landraces and modern cultivars, reaching nearly 100%. However, this increase was not observed in *japonica* varieties, suggesting that *OsTPS8* was a selective target during *indica* domestication (Fig. 6a). Furthermore, we validated the selection at the sequence level using F_{ST}, nucleotide diversity (π) and π ratio. Sequence comparison based on F_{ST} indicated a clear differentiation in the *OsTPS8* region between *indica* and *japonica*

Fig. 5 | Natural variation in the *OsTPS8* promoter affects the binding of OsbHLH001. a, Natural variation and haplotype analysis of *OsTPS8* in 331 Asian cultivated rice accessions. The black triangles represent natural variations; the red triangles represent functional natural variations between the $OsTPS8^{ASO}$ and $OsTPS8^{IR24}$ haplotypes. NA indicates an unknown correlation coefficient with the TopSite. **b**, Chalky grain percentage comparison of 331 Asian cultivated rice accessions carrying $OsTPS8^{ASO}$ ($n = 92$ independent rice accessions) and $OsTPS8^{IR24}$ ($n = 239$ independent rice accessions) haplotypes. **c**, Relative *OsTPS8* expression levels of the rice accessions carrying the $OsTPS8^{ASO}$ ($n = 16$ independent rice accessions) and $OsTPS8^{IR24}$ ($n = 18$ independent rice accessions) haplotypes in 12 DAF grains. **d**, Y1H assay between OsbHLH001 and the *OsTPS8* promoter. **e**, EMSA of the OsbHLH001 protein with the CAAGTG motif in the $OsTPS8^{C50}$ promoter. **f**, Transient expression assays of the transcriptional activity of OsbHLH001 on the -645 A/G site of the *OsTPS8* promoter in vivo ($n = 5$ biological replicates). **g**,**h**, Chalky grain percentage (**g**) and degree of chalkiness (**h**) of the *pGluC::OsbHLH001* lines at the C50 background ($n = 5$ plants). **i**, Architecture of pH-APOBEC1-SpRY construct and the corresponding mutant type and single-guide RNA (sgRNA) sequences. **j**, *OsTPS8* expression level, chalky grain percentage and degree of chalkiness of the PGE plants ($n = 5$ plants). Values are presented as the mean ± s.d (**b**,**c**,**f**–**h**,**j**). Statistical significance was determined using a two-tailed, paired Student's *t*-test (**b**,**c**,**g**,**h**,**j**). The different lowercase letters indicate significant differences ($P < 0.05$) based on a one-way ANOVA with Dunnet's multiple comparisons test (**f**). The Y1H, EMAS and transient expression assays were done independently three times with similar results.

https://doi.org/10.1038/s41588-025-02429-2

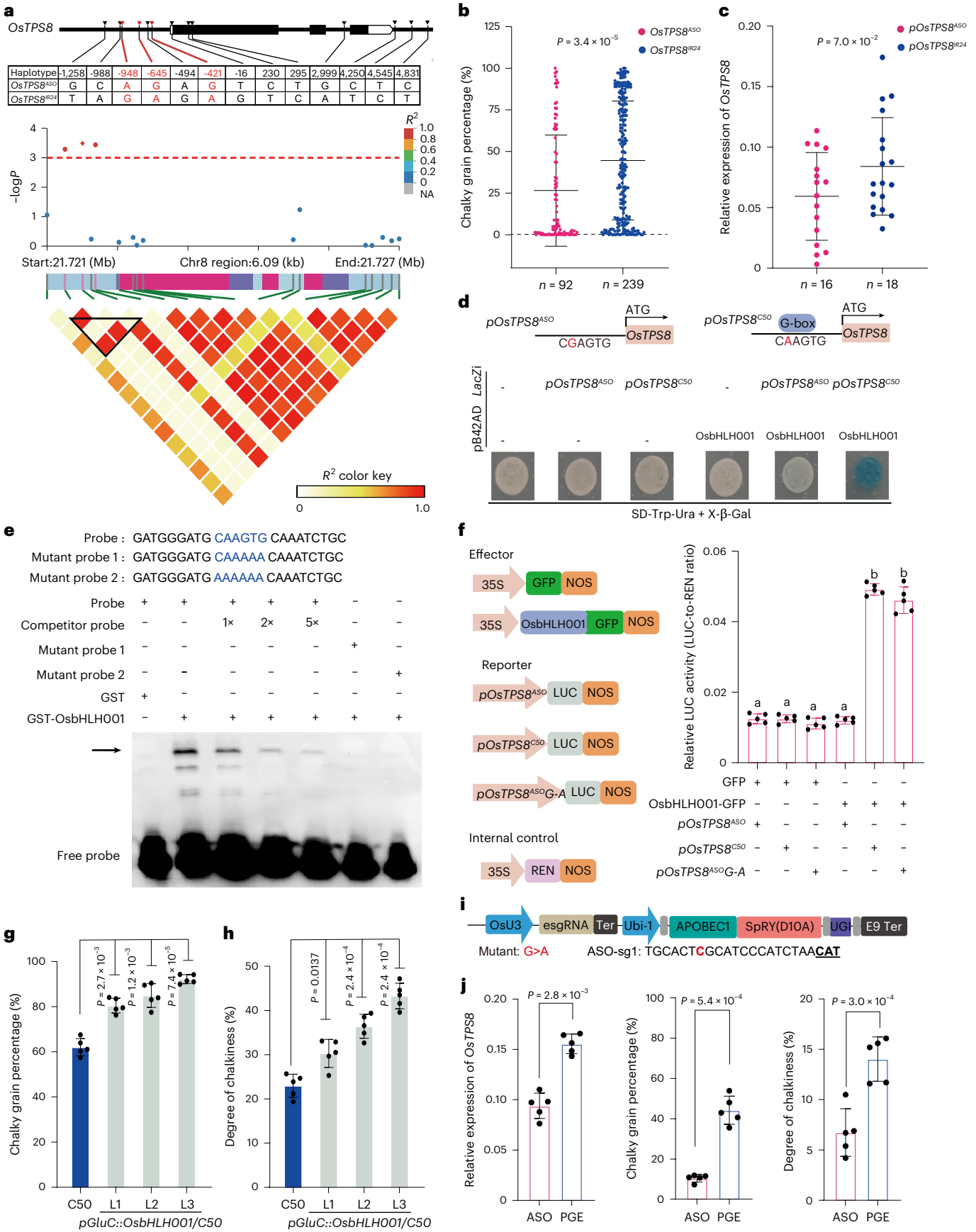

https://doi.org/10.1038/s41588-025-02429-2

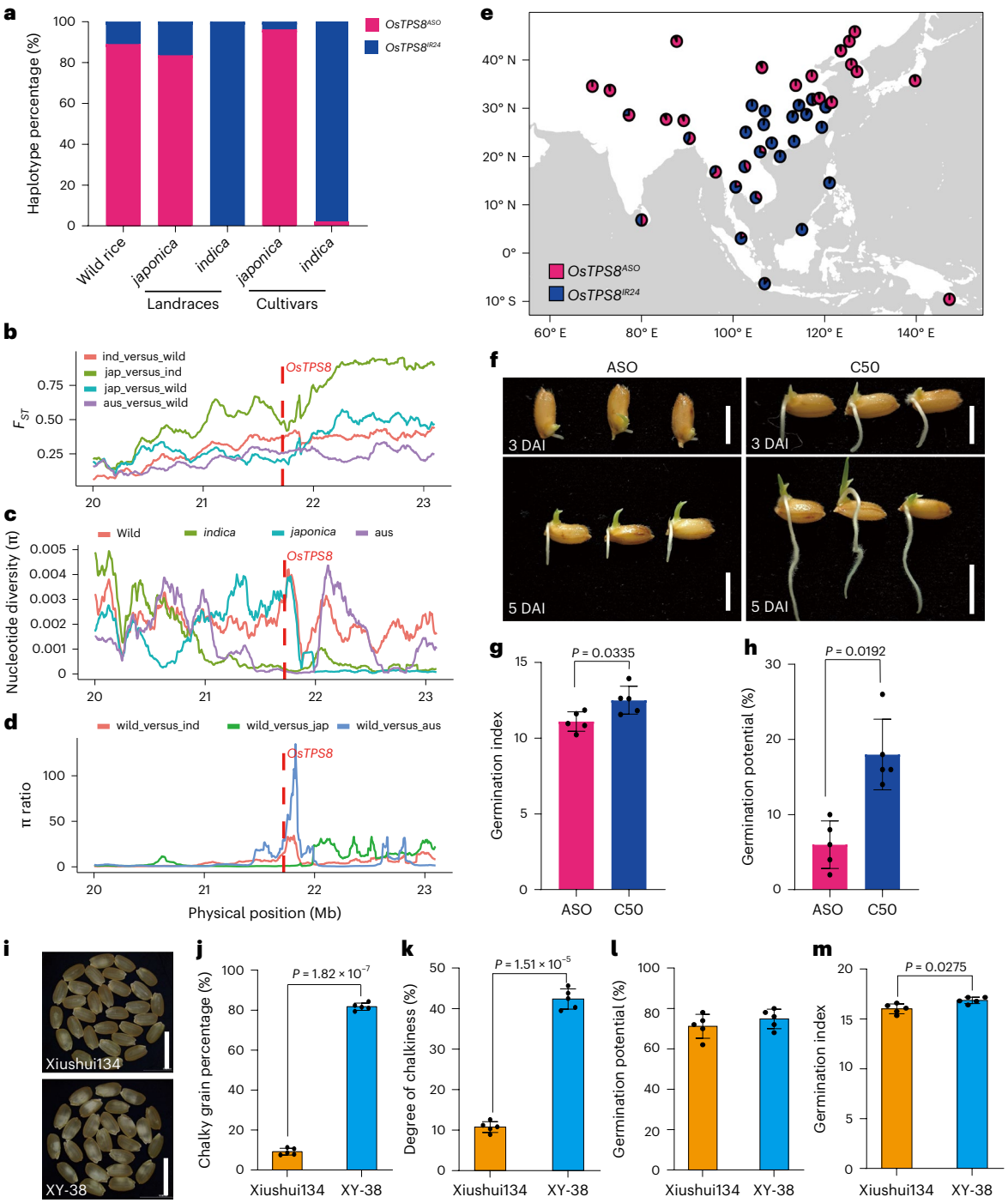

Fig. 6 | The *OsTPS8*^{IR24} allele improves seed vigor in *indica* cultivars. a, The frequency of *OsTPS8*^{ASO} and *OsTPS8*^{IR24} haplotypes in wild rice, landrace and cultivated rice accessions. **b**–**d**, F_{ST} (**b**), π (**c**) and π ratio (**d**) in wild rice and landraces across the 3-Mb genomic region of the *OsTPS8* locus. **e**, Geographical distribution of *OsTPS8*^{ASO} and *OsTPS8*^{IR24} among rice accessions in landraces and Chinese cultivars, depicted using the R package rnaturalearth with a base map sourced from Natural Earth (www.naturalearthdata.com). **f**, Germinated seeds of ASO and C50 at 3 and 5 DAI. **g**,**h**, Germination index (**g**) and germination potential (**h**) of ASO and C50 ($n = 5$ biological replicates). **i**, Observations of mature grains of Xiushui134 and the CSSL line XY-38. **j**,**k**, Chalky grain percentage (**j**) and degree of chalkiness (**k**) of Xiushui134 and XY-38 mature grains ($n = 5$ plants). **l**,**m**, Germination index (**l**) and germination potential (**m**) of Xiushui134 and XY-38 ($n = 5$ biological replicates). Values are presented as the mean ± s.d (**g**,**h**,**j**–**m**). Statistical significance was determined using a two-tailed, paired Student's *t*-test (**g**,**h**,**j**–**m**). Scale bar, 1 cm (**f**,**i**).

(Fig. 6b). The π value of the *OsTPS8* region was significantly decreased in the *indica* population, leading to a higher π ratio compared to wild rice populations (Fig. 6c,d). These results indicate that *OsTPS8*^{IR24} is artificially selected during the domestication of *indica* rice.

To explore the possible driving force underlying the selection of *OsTPS8*^{IR24} in *indica* rice, we conducted an analysis of the geographical distribution of landraces and cultivars. The results revealed that *OsTPS8*^{IR24} was predominantly distributed at low latitudes, particularly in regions such as Thailand, Malaysia, Vietnam and South China, which are usually direct seeding rice (DSR) growing areas[32] (Fig. 6e). The most important characteristic of DSR is fast germination[33]. Previous studies showed that Tre6P integrates sugar signaling and hormone

pathways to regulate seed germination[29,34]. Thus, we reasoned that *OsTPS8*^{IR24} might have been selected because of its higher seed vigor. Consistently, β-glucuronidase (GUS) staining showed high expression of *OsTPS8* in the embryo and embryonic roots during seed germination (Extended Data Fig. 5a). Phenotypic evaluation demonstrated that C50 exhibited higher germination speed and seedling growth under normal conditions (Fig. 6f and Extended Data Fig. 5b–g). The germination index and germination potential of C50 were significantly increased; thus, C50 possesses higher seed vigor than ASO (Fig. 6g,h). Moreover, both transgenic lines with elevated expression of *OsTPS8* and the PGE lines also exhibited higher seed vigor compared to WT, supporting the notion that *OsTPS8* positively regulates seed germination (Extended Data Fig. 6).

To further verify this notion, we obtained one CSSL line (XY-38) that introgressed the *indica* allele of *OsTPS8* from 9311 (*OsTPS8*^{IR24} variety) into Xiushui134 (*OsTPS8*^{ASO} variety). Compared to Xiushui134, XY-38 showed a significant increase in chalky grain percentage and degree of chalkiness (Fig. 6i–k), as well as higher seed vigor and seedling growth (Fig. 6l,m and Supplementary Fig. 11). Moreover, we randomly selected 83 rice accessions and tested their germination. The results showed that the *OsTPS8*^{IR24} varieties exhibited higher seed vigor than those harboring the *OsTPS8*^{ASO} haplotype (Extended Data Fig. 7 and Supplementary Table 5). In summary, the *OsTPS8* ^{IR24} haplotype is responsible for high seed vigor.

To demonstrate whether the difference in seed vigor caused by *OsTPS8* was also mediated by elevated starch degradation, we detected the soluble sugar content during seed germination. Our results showed that in the *OsTPS8* overexpression lines, soluble sugars were significantly higher than ASO at 24 and 48 h after imbibition (Extended Data Fig. 8a–c), although no significant differences were detected between the ASO, C50 and the PGE lines during germination, except for fructose at 48 h after imbibition (Supplementary Fig. 12). Consistently, we also found that the soluble sugar levels in germinating seeds of rice varieties carrying *OsTPS8*^{IR24} at 48 h after imbibition were significantly higher than the varieties carrying *OsTPS8*^{ASO} (Extended Data Fig. 8d,e).

Discussion

Indica and *japonica* rice are known to have distinct characteristics in grain chalkiness and seed vigor, two agronomic traits important for consumption and rice production, respectively[15,23]. However, little is known about their relationship and regulatory mechanisms. In this study, we demonstrated that the natural variation in *OsTPS8* confers differential regulation of grain chalkiness and seed vigor in the two subspecies of Asian cultivated rice. In this study, we propose a working model depicting the differential regulation of these two traits (Extended Data Fig. 9). According to this model, rice varieties of the *OsTPS8*^{IR24} haplotype (predominantly *indica*) have higher expression of *OsTPS8* because of differential binding by OsbHLH001. Increased *OsTPS8* transcripts in rice harboring the *OsTPS8*^{IR24} haplotype reduce the production of Tre6P, consequently resulting in higher expression of *OsMYBS1* and α-amylase genes, leading to elevated starch degradation and ultimately high chalkiness in rice grains. On the other hand, elevated starch degradation in *OsTPS8*^{IR24} rice provides more energy (Extended Data Fig. 8) and thus promotes seed vigor during germination[35]. Therefore, our findings uncover an OsbHLH001-OsTPS8-Tre6P-α-amylase signaling cascade that has a dual role in regulating both grain chalkiness and seed vigor in the two subspecies of Asian cultivated rice.

It is widely conceived that Tre6P could function as a signal and regulator of sucrose levels to affect plant growth and development, and stress tolerance[36–38]. Nevertheless, how Tre6P levels are regulated in plants is largely unknown. In this study, we found that OsTPS8 negatively regulates Tre6P production through interacting with OsTPS1 and inhibiting its catalytic activity (Fig. 3). Moreover, we found that Tre6P affects chalkiness and seed vigor by regulating the expression of *OsMYBS1* and α-amylase genes (Fig. 4). Nevertheless, how Tre6P exactly functions as a signal to regulate the expression of *OsMYBS1* and α-amylase genes remains unclear. A previous study reported that SnRK1 is necessary for the activation of *OsMYBS1* and *αAmy3* expression under glucose starvation[39]. Other studies have shown that Tre6P directly binds to KIN10 (a catalytic subunit of SnRK1) to inhibit the activation of SnRK1 (ref. 40). Thus, we speculate that the regulation of *OsMYBS1* and α-amylase gene expression by Tre6P may also entail SnRK1, a possibility awaiting to be investigated in future studies.

It is generally accepted that both *indica* and *japonica* rice were domesticated from the wild rice species *O. rufipogon*. During domestication, *indica* was adapted to the tropical regions in low latitudes, while temperate *japonica* rice was adapted to temperate regions at fairly high latitudes[2,41]. Our findings that almost all *indica* rice varieties carry the *OsTPS8*^{IR24} haplotype and that such rice germinates more rapidly than those with the *OsTPS8*^{ASO} haplotype (Fig. 6 and Extended Data Fig. 7) suggest that *OsTPS8*^{IR24} was probably selected during *indica* rice domestication because of its higher seed vigor, which allows more rapid seed germination, uniform seedling establishment and more effective competition with weeds. Moreover, higher seed vigor is also a beneficial trait for DSR, which has been adopted as the principal rice establishment method in the low latitudes of Southeast Asia and South China[32]. Our results also suggest that higher chalkiness in *indica* rice carrying the *OsTPS8*^{IR24} haplotype was probably intentionally neglected during domestication and breeding improvement at the cost of selecting for higher seed vigor. Notably, previous studies repeatedly identified QTLs for low-temperature germination traits near or even covering the *OsTPS8* locus[42,43], hinting at a possibility for retaining the *OsTPS8*^{ASO} haplotype in *japonica* rice for low-temperature germination. Typical *indica* rice has long grains and *japonica* rice has short and round grains. Dozens of studies demonstrated that an increase in the grain length-to-width ratio is associated with a decrease in chalkiness[44,45]. Therefore, pyramiding slender grain genes such as *gs3*, *gs5*, *GW5* and *gw7* with *OsTPS8*^{IR24} is expected to reduce grain chalkiness and retain high seed vigor, while meeting the demands of both market and production. Our findings that the natural variation in the promoter of *OsTPS8* contributes to the differentiation of grain chalkiness and seed vigor between *indica* and *japonica* subspecies provides a candidate gene for the improvement of both grain appearance quality and seed vigor in rice.

Online content

Any methods, additional references, Nature Portfolio reporting summaries, source data, extended data, supplementary information, acknowledgements, peer review information; details of author contributions and competing interests; and statements of data and code availability are available at https://doi.org/10.1038/s41588-025-02429-2.

References

1. Wing, R. A., Purugganan, M. D. & Zhang, Q. The rice genome revolution: from an ancient grain to Green Super Rice. *Nat. Rev. Genet.* **19**, 505–517 (2018).
2. Wang, X. et al. Selective and comparative genome architecture of Asian cultivated rice (*Oryza sativa* L.) attributed to domestication and modern breeding. *J. Adv. Res.* **42**, 1–16 (2022).
3. Wang, W., Gao, H., Liang, Y., Li, J. & Wang, Y. Molecular basis underlying rice tiller angle: Current progress and future perspectives. *Mol. Plant* **15**, 125–137 (2022).
4. Gou, Y. et al. Natural variation in *OsMYB8* confers diurnal floret opening time divergence between *indica* and *japonica* subspecies. *Nat. Commun.* **15**, 2262 (2024).
5. Yan, Y., Zhu, X., Qi, H., Zhang, H. & He, J. Regulatory mechanism and molecular genetic dissection of rice (*Oryza sativa* L.) grain size. *Heliyon* **10**, e27139 (2024).
6. Hu, B., Wang, W., Chen, J., Liu, Y. & Chu, C. Genetic improvement toward nitrogen-use efficiency in rice: lessons and perspectives. *Mol. Plant* **16**, 64–74 (2023).

7. Zhao, D., Zhang, C., Li, Q. & Liu, Q. Genetic control of grain appearance quality in rice. *Biotechnol. Adv.* **60**, 108014 (2022).
8. Deng, F. et al. Relationship between chalkiness and the structural and thermal properties of rice starch after shading during grain-filling stage. *Carbohydr. Polym.* **252**, 117212 (2021).
9. Chen, Z. et al. Dry cultivation and cultivar affect starch synthesis and traits to define rice grain quality in various panicle parts. *Carbohydr. Polym.* **269**, 118336 (2021).
10. Guo, C. et al. Nitrogen application rate affects the accumulation of carbohydrates in functional leaves and grains to improve grain filling and reduce the occurrence of chalkiness. *Front. Plant Sci.* **13**, 921130 (2022).
11. Park, J.-R., Kim, E.-G., Jang, Y.-H. & Kim, K.-M. Screening and identification of genes affecting grain quality and spikelet fertility during high-temperature treatment in grain filling stage of rice. *BMC Plant Biol.* **21**, 263 (2021).
12. Li, Y. et al. *Chalk5* encodes a vacuolar H^+-translocating pyrophosphatase influencing grain chalkiness in rice. *Nat. Genet.* **46**, 398–404 (2014).
13. Wu, B. et al. Natural variation in *WHITE-CORE RATE 1* regulates redox homeostasis in rice endosperm to affect grain quality. *Plant Cell* **34**, 1912–1932 (2022).
14. Yang, W. et al. OsbZIP60-mediated unfolded protein response regulates grain chalkiness in rice. *J. Genet. Genomics* **49**, 414–426 (2022).
15. Feng, F., Li, Y., Qin, X., Liao, Y. & Siddique, K. H. M. Changes in rice grain quality of *indica* and *japonica* type varieties released in China from 2000 to 2014. *Front. Plant Sci.* **8**, 1863 (2017).
16. Huo, X. et al. Genome-wide association mapping and gene expression analysis reveal candidate genes for grain chalkiness in rice. *Front. Plant Sci.* **14**, 1184276 (2023).
17. Reed, R. C., Bradford, K. J. & Khanday, I. Seed germination and vigor: ensuring crop sustainability in a changing climate. *Heredity* **128**, 450–459 (2022).
18. Finch-Savage, W. E. & Bassel, G. W. Seed vigour and crop establishment: extending performance beyond adaptation. *J. Exp. Bot.* **67**, 567–591 (2016).
19. He, Y. et al. *OsHIPL1*, a hedgehog-interacting protein-like 1 protein, increases seed vigour in rice. *Plant Biotechnol. J.* **20**, 1346–1362 (2022).
20. Yang, B. et al. Identification of *OsPK5* involved in rice glycolytic metabolism and GA/ABA balance for improving seed germination via genome-wide association study. *J. Exp. Bot.* **73**, 3446–3461 (2022).
21. Li, W. et al. A genome-wide association study reveals that the 2-oxoglutarate/malate translocator mediates seed vigor in rice. *Plant J.* **108**, 478–491 (2021).
22. Zhao, J., He, Y., Huang, S. & Wang, Z. Advances in the identification of quantitative trait loci and genes involved in seed vigor in rice. *Front. Plant Sci.* **12**, 659307 (2021).
23. Wang, Z., Wang, J., Bao, Y., Wang, F. & Zhang, H. Quantitative trait loci analysis for rice seed vigor during the germination stage. *J. Zhejiang Univ. Sci. B* **11**, 958–964 (2010).
24. Guo, T. et al. Identification of a stable quantitative trait locus for percentage grains with white chalkiness in rice (*Oryza sativa*). *J. Integr. Plant Biol.* **53**, 598–607 (2011).
25. Huang, L., Tan, H., Zhang, C., Li, Q. & Liu, Q. Starch biosynthesis in cereal endosperms: an updated review over the last decade. *Plant Commun.* **2**, 100237 (2021).
26. Zang, B., Li, H., Li, W., Deng, X. W. & Wang, X. Analysis of trehalose-6-phosphate synthase (TPS) gene family suggests the formation of TPS complexes in rice. *Plant Mol. Biol.* **76**, 507–522 (2011).
27. Chen, X. et al. Trehalose phosphate synthase complex-mediated regulation of trehalose 6-phosphate homeostasis is critical for development and pathogenesis in *Magnaporthe oryzae*. *mSystems* **6**, e0046221 (2021).
28. Nakata, M. et al. High temperature-induced expression of rice α-amylases in developing endosperm produces chalky grains. *Front. Plant Sci.* **8**, 2089 (2017).
29. Kretzschmar, T. et al. A trehalose-6-phosphate phosphatase enhances anaerobic germination tolerance in rice. *Nat. Plants* **1**, 15124 (2015).
30. Xu, F. et al. Antagonistic control of seed dormancy in rice by two bHLH transcription factors. *Nat. Genet.* **54**, 1972–1982 (2022).
31. Jing, C.-Y. et al. Multiple domestications of Asian rice. *Nat. Plants* **9**, 1221–1235 (2023).
32. Chaudhary, A., Venkatramanan, V., Kumar Mishra, A. & Sharma, S. Agronomic and environmental determinants of direct seeded rice in South Asia. *Circ. Econ. Sustain.* **3**, 253–290 (2023).
33. Mahender, A., Anandan, A. & Pradhan, S. K. Early seedling vigour, an imperative trait for direct-seeded rice: an overview on physio-morphological parameters and molecular markers. *Planta* **241**, 1027–1050 (2015).
34. Wang, G. et al. *OsTPP1* regulates seed germination through the crosstalk with abscisic acid in rice. *New Phytol.* **230**, 1925–1939 (2021).
35. Ma, M., Xu, Y., Liu, Z., Sui, Z. & Corke, H. Removal of starch granule-associated proteins promotes α-amylase hydrolysis of rice starch granule. *Food Chem.* **330**, 127313 (2020).
36. Fichtner, F. & Lunn, J. E. The role of trehalose 6-phosphate (Tre6P) in Plant metabolism and development. *Annu. Rev. Plant Biol.* **72**, 737–760 (2021).
37. Nuccio, M. L. et al. Expression of trehalose-6-phosphate phosphatase in maize ears improves yield in well-watered and drought conditions. *Nat. Biotechnol.* **33**, 862–869 (2015).
38. Vishal, B., Krishnamurthy, P., Ramamoorthy, R. & Kumar, P. P. *OsTPS8* controls yield-related traits and confers salt stress tolerance in rice by enhancing suberin deposition. *New Phytol.* **221**, 1369–1386 (2019).
39. Lu, C.-A. et al. The SnRK1A protein kinase plays a key role in sugar signaling during germination and seedling growth of rice. *Plant Cell* **19**, 2484–2499 (2007).
40. Zhai, Z. et al. Trehalose 6-phosphate positively regulates fatty acid synthesis by stabilizing WRINKLED1. *Plant Cell* **30**, 2616–2627 (2018).
41. Wang, W. et al. Genomic variation in 3,010 diverse accessions of Asian cultivated rice. *Nature* **557**, 43–49 (2018).
42. Zhang, Z.-H., Qu, X.-S., Wan, S., Chen, L.-H. & Zhu, Y.-G. Comparison of QTL controlling seedling vigour under different temperature conditions using recombinant inbred lines in rice (*Oryza sativa*). *Ann. Bot.* **95**, 423–429 (2005).
43. Pan, Y. et al. Genetic analysis of cold tolerance at the germination and booting stages in rice by association mapping. *PLoS ONE* **10**, e0120590 (2015).
44. Wang, Y. et al. Copy number variation at the *GL7* locus contributes to grain size diversity in rice. *Nat. Genet.* **47**, 944–948 (2015).
45. Zhao, D.-S. et al. *GS9* acts as a transcriptional activator to regulate rice grain shape and appearance quality. *Nat. Commun.* **9**, 1240 (2018).

Methods

Material growth and phenotyping

C50 was derived from the CSSL population constructed using IR24 and Asominori. The experimental materials were all planted in Nanjing (119° E, 32° N) and Hainan (110° E, 18° N) experimental stations of Nanjing Agricultural University, China. The chalky grain percentage of brown rice was counted manually, and the degree of chalkiness was measured using a rice appearance quality detector (JMWT12, SATAKE). Ten plants were selected for the investigation of agronomic traits. Determination of grain nutrients (starch, protein and lipid) followed previously published methods[46]. For the single-gene association analysis, 331 Asian cultivated rice accessions were planted in 2019 and 2020 in Hainan, China. All plant materials were grown under standard agronomic conditions.

Microscopic observation

For transmission electron microscopy, transverse sections of the mature grains were sputter-coated with gold powder and observed with a Hitachi Regulus 8100 scanning electron microscope. For semi-thin section observation, samples approximately 1-mm thick from the middle part of the developing endosperm were fixed, dehydrated and embedded in LR White resin (London Resin). Semi-thin (1-μm) sections were cut, stained with 1% iodine-potassium iodide and photographed with a light microscope (ECLIPSE80i, Nikon)[46].

Map-based cloning

First, *qPGWC-8* for the chalky grain percentage was located between 8G-7 and 8G-9 on the long arm of chromosome 8 (ref. 24). Then, fine-mapping was conducted using 7,910 individuals, narrowing down the interval to a 35-kb region between 8G-7 and 8G-32. Progeny tests were performed on all recombinant individuals used for fine-mapping. The markers used in this study are listed in Supplementary Table 6.

Vector construction and rice transformation

For the transgenic vectors, a 2-kb promoter fragment of *OsTPS8* was fused with the 5-kb genomic coding regions. The recombinant fragments were inserted into the pCAMBIA1300 vector using homologous recombination. For GFP-tagged *OsTPS8* transgenic plants, the coding sequence (CDS) of *OsTPS8* was cloned into the pCAMBIA1305-GFP vector to generate the *pOsTPS8::OsTPS8-GFP* construct. For the spatiotemporal expression analysis, the promoter region of *OsTPS8* (2 kb upstream of ATG) was recombined into pCAMBIA1381Z. For base editing, a tiled sgRNA was designed to target the promoter of *OsTPS8*. Annealed oligonucleotides were inserted into BsaI-digested (New England BioLabs) pH-APOBEC1-SpRY vectors[47]. The *OsTPS8* KO construct was prepared by inserting a 20-bp target sequence in the first exon into the CRISPR–Cas9 vector. Recombinant vectors were transformed into the *Agrobacterium tumefaciens* strain EHA105 and used to infect the rice calli of ASO or C50. The primers used in this study are listed in Supplementary Table 6.

RNA extraction and RT–qPCR

Total RNA was extracted from several plant tissues using an RNA extraction kit (Tiangen Biotech). The first-strand complementary DNA was synthesized using the HiScript Ⅱ 1st Strand cDNA Synthesis Kit (cat. no. R212-02, Vazyme). RT–qPCR assays were performed on a T100TM real-time PCR system (Bio-Rad Laboratories) with the Genious 2X SYBR Green Fast qPCR Mix (cat. no. RM21204, ABclonal). The rice *UBIQUITIN* gene was used as an internal control. The relative gene expression level was calculated using the $2^{-\Delta\Delta C_T}$ method. *P* values were calculated using a two-sided paired Student's *t*-test. The RT–qPCR primers used in this study are listed in Supplementary Table 6.

Subcellular localization

To determine the subcellular localization of OsTPS8, rice protoplasts were isolated from 10-day-old seedlings of the *pOsTPS8::OsTPS8-GFP* transgenic lines. Fluorescence signals were observed using a confocal laser scanning microscope (TCS-SP8, Leica Microsystems). For fractionation, developing grains of the *pOsTPS8::OsTPS8-GFP* transgenic lines were used as described previously[48]. Nine DAF grains were homogenized on ice in buffer A (100 mM HEPES-KOH, pH 7.5, 0.3 M sucrose, 5 mM EGTA, 5 mM $MgCl_2$ and protease inhibitor cocktail (cat. no. C600384, Sangon Biotech)). The homogenate was filtered through a magic filter cloth and centrifuged at 50*g* for 30 min to remove starch; the supernatant was retained as total protein (T). Subsequently, the supernatant was further centrifuged at 2,000*g* for 20 min at 4 °C to obtain the supernatant (S2) and pellet (P2) fractions. Then, the S2 fraction was further centrifuged at 13,000*g* and 100,000*g* to obtain the S13, P13, S100 and P100 fractions for the immunoblot analysis.

GUS staining

The vector containing the CDS of *β-GUS* driven by the *OsTPS8* promoter was transformed into ASO. All plant tissues were stained according to the instructions of the GUS kit (cat. no. G3061, Solarbio). Stained samples were decolorized with graded alcohol and photographed with a stereoscope (Leica Application Suite 3.3).

Seed protein extraction, SDS–polyacrylamide gel electrophoresis and immunoblot analyses

The protein extraction and immunoblotting assays were conducted with slight modification as described previously[48]. Briefly, mature seeds or developing grains were crushed and then resuspended in lysis buffer. SDS–polyacrylamide gel electrophoresis analysis was performed using 4–20% (v/v) precast gels (cat. no. M00655, Genscript), followed by staining with Coomassie brilliant blue or immunoblot analyses. Synthetic peptides of OsTPS8 (LOC_Os08g34580; PSLPNSGDEGGA and RQEGPVPTAPAGKPRQ) and amylase (LOC_Os08g36900; PGRLYDLDASKYG and FEGGTPDGRLDWGP, two highly homologous peptides of the α-amylase protein family) were synthesized. The synthetic peptides were injected to rabbits to generate polyclonal antibodies at ABclonal Biotechnology (www.abclonal.com.cn/). EF-1α was previously described in ref. 45. Anti-GFP (11814460001, Roche), anti-FLAG (cat. no. A8592, Sigma-Aldrich), anti-GST (cat. no. PM013-7, MBL Life Science), anti-H3 (cat. no. ab1791, Abcam) and anti-cFBPase (cat. no. AS04 043, Agrisera) antibodies are commercially available. Immunoblotting signals were detected with the ECL detection reagent (cat. no. 32209, Thermo Fisher Scientific).

Y1H experiment

The Y1H assay was performed according to previously described methods[49]. The *OsbHLH001* CDS and *OsTPS8* promoters of different haplotypes (-1 kb upstream of ATG) were connected to the pB42AD and pLacZi vectors, respectively. The SD-Trp-Ura medium was used to screen positive clones, which were cotransformed into the EGY48 yeast strain. The positive transformants were transferred to SD-Trp-Ura plates with X-β-Gal to verify the interaction.

EMSA

The *OsbHLH001* CDS was inserted into the pGEX-4T-2 vector and transformed into the *DE3* strain for prokaryotic expression. Expressed GST-OsbHLH001 fusion protein was purified according to the manufacturer's instructions (cat. no. L00207, Genscript). For EMSA, a 5′ biotin-modified 24-bp sequence containing the CANNTG motif was selected as the probe; the unlabeled probe was used as the competitive probe. Two mutant probes with sequences replaced with either CAAAAA or AAAAAA were used. The GST-OsbHLH001 fusion protein was purified for EMSA with the probes. The unlabeled competitive probe was added in onefold, twofold and fivefold molar excess. Gel migration was performed according to the manufacturer's protocol (cat. no. 89880, Thermo Fisher Scientific).

Dual-LUC reporter assay

For the promoter activity assay, the two parental promoters and A/G mutation-type promoters of *OsTPS8* were cloned into the pGreen II 0800-LUC plasmid; *OsbHLH001* was recombined into the pAN580 vector. Various combinations of recombinant plasmids were cotransformed into rice protoplasts, followed by incubation in the dark at 28 °C for more than 16 h. The firefly LUC and REN activities were measured according to the manufacturer's instructions (cat. no. E1910, Promega Corporation) using a chemiluminescence detector (GloMax 20/20, Promega Corporation).

For the transcriptional repression of the α-amylase genes and *OsMYBS1* by Tre6P, the promoter of *OsAmy3D* or *OsMYBS1* was recombined into the pGreen II 0800-LUC plasmid (*pOsAmy3D::LUC* or *pOsMYBS1::LUC*). High-purity plasmids were transformed into rice protoplasts and cultured in the dark at 28 °C for 12 h. Subsequently, Tre6P was added at several concentrations and incubated for different times. The LUC and REN values were determined according to the method described above. Extraction of protoplast RNA and RT–qPCR were conducted as described above.

LCI assays

The CDSs of *OsTPS8* and *OsTPS1* were cloned into the nLUC and cLUC vectors, respectively. These plasmids were transformed into *A. tumefaciens* strain EHA105. Different combinations of these constructs were prepared and transformed into the leaf epidermal cells of *Nicotiana benthamiana* and cultured for 24–48 h. The fluorescence signals were collected with a fully automatic chemiluminescence imaging system (Tanon-5200).

Co-IP assays

The CDSs of *OsTPS1* and *OsTPS8* without stop codon were cloned into the pCAMBIA1305-GFP and pCAMBIA1300-221-Flag vectors, respectively. These constructs were cotransformed into *N. benthamiana* for transient expression. Total protein was extracted with the NB1 buffer (Tris-MES, pH 7.4, 50 mM sucrose, 500 mM $MgCl_2$, 1 mM dithiothreitol, 5 mM EDTA, 10 mM Nonidet P-40 and 0.1% (v/v) and protease inhibitor cocktail). The protein extract was incubated at 4 °C for 30 min on a shaker. After centrifugation at 12,000*g* at 4 °C, the supernatant was incubated with FLAG-beads at 4 °C for 2 h. Then, the FLAG-beads were washed five times with extraction buffer. The FLAG-beads were boiled with protein loading buffer for 10 min and subjected to immunoblot assay as described above.

Determination of Tre6P content

Developing or mature grains were ground thoroughly with 80% methanol. After vortexing for 5 min, the homogenate was ultrasonically extracted at 100 W and 20 °C for 20 min. The extract was centrifuged at 12,000*g* at 4 °C for 20 min to obtain the supernatant, which was passed through a 0.22-μm water filter. The ACQUITY UPLC I-Class PLUS (Waters) system coupled with the Xevo TQ-S Micro MS/MS (Waters) was used for sample determination with the ACQUITY UPLC HSSC18 column (cat. no. 186002350). The mobile phase consisted of ultrapure water (A) and 100% methanol (B). The LC run time was 5 min using the following gradient elution profile: 0–0.2 min, 98% A solution, 2% B solution; 0.2–4 min, 100% B solution; and 4–5 min, 98% A solution, 2% B solution. The flow rate was 0.2 ml min^{-1}. The ion trap mass spectrometer was operated in the negative ion mode with a 2.5-kV capillary voltage and an ion source temperature of 150 °C. Tre6P was detected as deprotonated molecules at 421.05 > 78.863 *m/z*.

Yeast complementation assays

The specific experimental method has been described in a previous report[26]. The yeast strains used in this study include WT strain W303-1A as well as the *tps1* and *tps2* mutant strains. Specifically, the *tps1* mutant strain was transformed only with the *OsTPS8* or *OtsA* (positive control) genes and spotted on leucine-free minimal medium (SD-Leu) supplemented with 2% galactose or 2% glucose as indicated. Similarly, the *tps2* mutant strain was transformed with the *OsTPS8* or *OtsB* (positive control) genes. All yeast transformants were grown on SD-Leu containing 2% glucose at 30 °C and 38.6 °C. The WT strain was transformed with the pGAL vector.

Enzymatic activity assays

OsTPS1-GFP was expressed in the protoplasts of the *OsTPS8* KO plants and purified by GFP magnetic beads. GST-OsTPS8 was purified as described above. The enzymatic activity of the TPS complexes was assessed by measuring the content of Tre6P generated from glucose-6-phosphate. Purified proteins were added to the reaction buffer (Tris-HCl, pH 7.5, 20 mM glucose-6-phosphate, 10 mM UDP-glucose, 0.04 mg heparin ml^{-1} and 10 mM $MgCl_2$) and incubated at 37 °C for 20 min. The sample was then boiled for 5 min. Denatured proteins were removed using centrifugation. Tre6P contents were determined using liquid chromatography–mass spectrometry. α-Amylase activity was determined using the α-Amylase kit from Megazyme (K-CERA) according to the manufacturer's instructions.

Evaluation of seed vigor

Thirty seeds per replicate of ASO, C50, transgenic lines and rice accessions were imbibed in 9-cm-diameter Petri dishes with 10 ml distilled water at 30 °C for 7 days. Seed germination was defined as the coleoptile having emerged to the half-length of the seed. The traits of seed vigor, including germination potential and germination index, were tested according to ref. 50. The percentage of germinated seeds 3 days after imbibition (DAI) is referred to as the germination potential. The germination index is calculated as follows: $GI = \sum (Gt/t)$, where Gt is the number of the germinated seeds on day t. Five replications were performed. Meanwhile, 30 seeds per replicate were sowed in soil under controlled conditions. They were cultivated in an artificial incubator under 16 h light and 8 h dark at 30 °C during the day and 25 °C at night. Seeds were collected and dried at 45 °C for 7 days to break seed dormancy.

Statistics and reproducibility

All quantitative data are presented as the mean ± s.d. from at least three independent experiments. Sample sizes (n) and P values are shown in each figure and figure legend. P values were derived using a two-tailed Student's t-test. Statistical significance was determined using a one-way analysis of variance (ANOVA) with Dunnet's multiple comparisons test using SPSS.

Different letters represent significant differences ($P < 0.05$). Results with a $P < 0.05$ were considered statistically significant. LUC reporter, Y1H, EMSA and Y2H assays, co-IP, GST pull-down, the LCI assay, subcellular localization, confocal microscopy and two-phase partitioning were done independently at least three times with similar results. Single-gene association analysis was performed using the GWAS-rMVP R package with the GLM algorithm[51]. LDBlockShow v.1.40 was used to carry out the pairwise linkage disequilibrium analysis of the *OsTPS8*-related genomic region[51]. For the phylogenetic analysis of *OsTPS8*, the genomic sequences of 1,453 rice accessions were obtained from ref. 31; they consisted of 359 wild accessions and 1,094 rice landraces[31]. Geographical distribution of the sampling sites were plotted using the R package rnaturalearth, based on a base map from Natural Earth (www.naturalearthdata.com). The π and F_{ST} in *OsTPS8* and the flanking regions (~3 Mb) for each rice group were calculated using VCFtools (https://vcftools.github.io/), using a 100-kb window with a step size of 5 kb. No statistical method was used to predetermine sample size. Data distribution was assumed to be normal, but this was not formally tested

Reporting summary

Further information on research design is available in the Nature Portfolio Reporting Summary linked to this article.

Data availability

The data supporting the findings of this study are available in the article and its Supplementary Information. For the phylogenetic analysis of *OsTPS8*, the genomic sequences of 1,453 rice accessions (359 wild accessions and 1,094 rice landraces) were obtained from Jing et al.[31]. The sequence data used in this study can be accessed at the GenBank/EMBL databases: *OsTPS8*/*Os08g0445700* (www.ncbi.nlm.nih.gov/gene/?term=LOC4345706), *OsAmy1A*/*Os02g0765600* (www.ncbi.nlm.nih.gov/gene/?term=LOC4330832), *OsAmy1C*/*Os02g0765400* (www.ncbi.nlm.nih.gov/gene/?term=LOC4330830), *OsAmy2A*/*Os06g0713800* (www.ncbi.nlm.nih.gov/gene/?term=LOC4342055), *OsAmy3A*/*Os09g0457400* (www.ncbi.nlm.nih.gov/gene/?term=LOC4347262), *OsAmy3B*/*Os09g0457600* (www.ncbi.nlm.nih.gov/gene/?term=LOC9271949), *OsAmy3C*/*Os09g0457800* (www.ncbi.nlm.nih.gov/gene/?term=LOC4347265), *OsAmy3D*/*Os08g0473900* (www.ncbi.nlm.nih.gov/gene/?term=LOC4345814), *OsAmy3E*/*Os08g0473600* (www.ncbi.nlm.nih.gov/gene/?term=LOC4345812), *OsMYBS1*/*Os01g0524500* (www.ncbi.nlm.nih.gov/gene/?term=LOC4323963) and *OsbHLH001*/*Os01g0928000* (www.ncbi.nlm.nih.gov/gene/?term=LOC4326959). The geographical distribution of sampling sites was plotted using the R package rnaturalearth based on a base map from Natural Earth (www.naturalearthdata.com). The code and source data for the bioinformatic analyses in this study have been deposited via Zenodo at https://doi.org/10.5281/zenodo.17393750 (ref. 52). Source data are provided with this paper.

Code availability

All software used in this study is publicly available as described in Methods and Reporting Summary. The customized scripts and codes used in the present study are available via Zenodo at https://doi.org/10.5281/zenodo.17393750 (ref. 52).

References

46. Chen, X. et al. Fructose-6-phosphate-2-kinase/fructose-2,6-bisphosphatase regulates energy metabolism and synthesis of storage products in developing rice endosperm. *Plant Sci.* **326**, 111503 (2023).
47. Zhang, A. et al. Directed evolution rice genes with randomly multiplexed sgRNAs assembly of base editors. *Plant Biotechnol. J.* **21**, 2597–2610 (2023).
48. Wang, Y. et al. GOLGI TRANSPORT 1B regulates protein export from the endoplasmic reticulum in rice endosperm cells. *Plant Cell* **28**, 2850–2865 (2016).
49. Lin, R. et al. Transposase-derived transcription factors regulate light signaling in *Arabidopsis*. *Science* **318**, 1302–1305 (2007).
50. He, Y. et al. Indole-3-acetate beta-glucosyltransferase *OsIAGLU* regulates seed vigour through mediating crosstalk between auxin and abscisic acid in rice. *Plant Biotechnol. J.* **18**, 1933–1945 (2020).
51. Dong, S.-S. et al. LDBlockShow: a fast and convenient tool for visualizing linkage disequilibrium and haplotype blocks based on variant call format files. *Brief. Bioinform.* **22**, bbaa227 (2021).
52. Jiang, X. Supporting code for OsTPS8 variation and selection analyses in rice. *Zenodo* https://doi.org/10.5281/zenodo.17393751 (2025).

Acknowledgements

We thank J. M. Thevelein at the Laboratory of Molecular Cell Biology, Institute of Botany and Microbiology, KU Leuven for the *Saccharomyces cerevisiae* W303-1A strain and the *tps1* and *tps2* mutant strains. We thank X. Wei at the China National Rice Research Institute for providing the XY-38 line. We also thank S. Ge at the Institute of Botany, Chinese Academy of Sciences for providing information on the genetic variations of wild rice germplasms. This study was supported by grants from the National Key Research and Development Program of China (no. 2022YFD1200101 to Yihua Wang), the 'JBGS' Project of the Seed Industry Revitalization in Jiangsu Province (nos. JBGS(2021)008 to Yihua Wang and JBGS(2021)035 to Y.T.), the Innovation Program of the Chinese Academy of Agricultural Sciences, the Fundamental Research Funds for the Central Universities (nos. KYT2024005 and KYZZ2024005 to Yihua Wang) and the National Natural Science Foundation of China (nos. 32272168 to Yunlong Wang, 32372164 to E.D. and 31921004 to J.W.). The work was also supported by the Key Laboratory of Biology, Genetics, and Breeding of *Japonica* Rice in the Mid-lower Chang Jiang (Yangtze River), Ministry of Agriculture, People's Republic of China, and the Jiangsu Collaborative Innovation Center for Modern Crop Production.

Author contributions

X.C., Y.R., H.D. and X.J. performed all the experiments and analyzed the data. X.Z., E.D., X.T., Yunlong Wang, C.G., R.C., Q.W., Yongfei Wang, Yipeng Zhang, R.Z., Yunpeng Zhang, W.Z., Yu Zhang, X.Y., L.Z., C.L., T.S., Y.B., Y.T., X.L., S.L., T.G. and M.C. provided technical support. J.W., Yihua Wang and H.W. supervised the project and wrote the paper.

Competing interests

The authors declare no competing interests.

Additional information

Extended data is available for this paper at https://doi.org/10.1038/s41588-025-02429-2.

Supplementary information The online version contains supplementary material available at https://doi.org/10.1038/s41588-025-02429-2.

Correspondence and requests for materials should be addressed to Haiyang Wang, Yihua Wang or Jianmin Wan.

Peer review information *Nature Genetics* thanks Yuqing He, Takeshi Izawa, Wenbin Zhou for their contribution to the peer review of this work. Peer reviewer reports are available.

https://doi.org/10.1038/s41588-025-02429-2

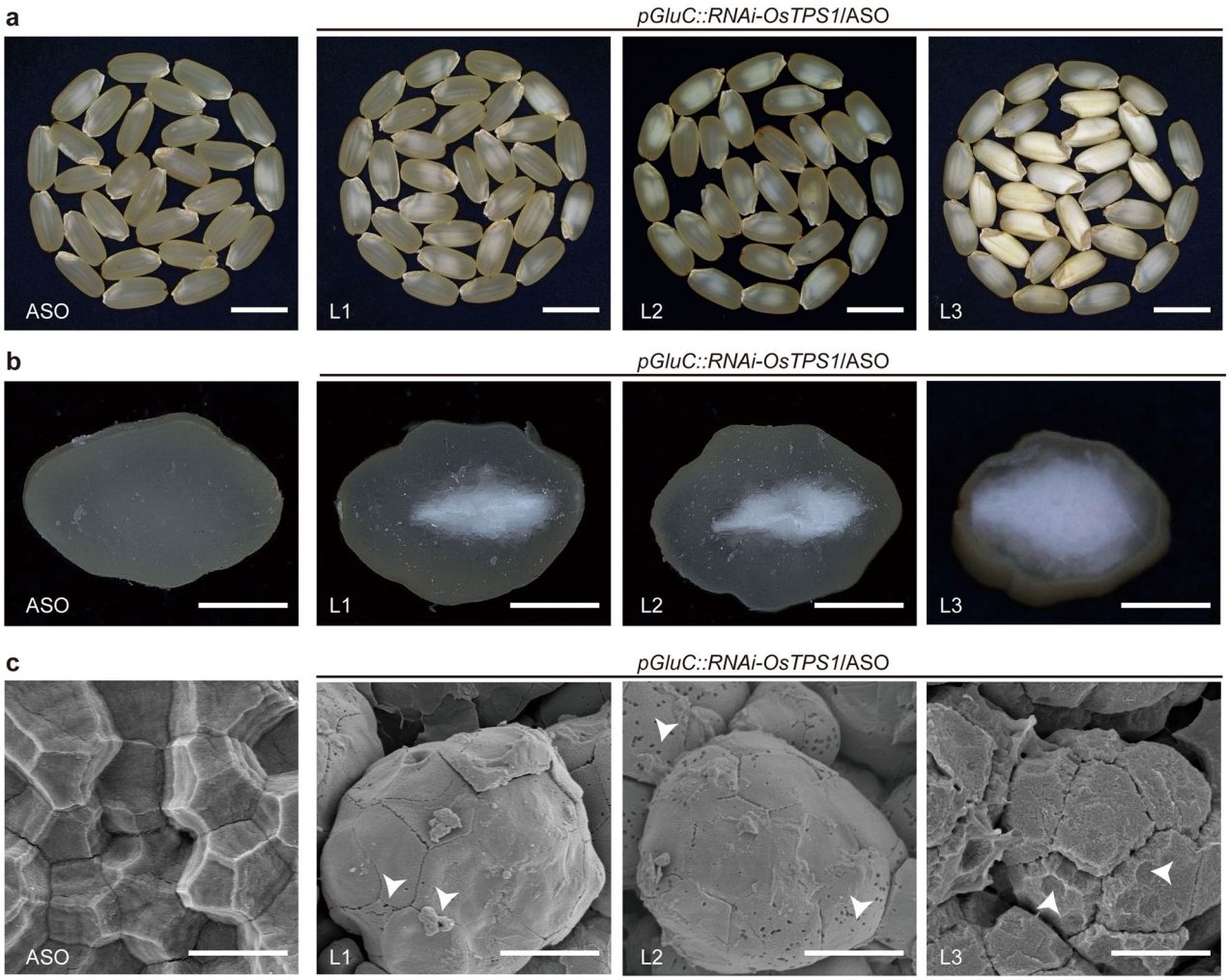

Extended Data Fig. 1 | Phenotypic characterization of the *pGluC::RNAi-OsTPS1* transgenic lines. a,**b**, Mature grains of ASO and the *pGluC::RNAi-OsTPS1* transgenic lines. Scale bars, 5 mm (**a**) and 1 mm (**b**). **c**, SEM observations of cross-sections of mature grains from ASO and the *pGluC::RNAi-OsTPS1* lines. White arrowheads indicate the holes on starch granules. Scale bars, 5 μm. L1, L2, and L3 represent three independent transgenic lines.

https://doi.org/10.1038/s41588-025-02429-2

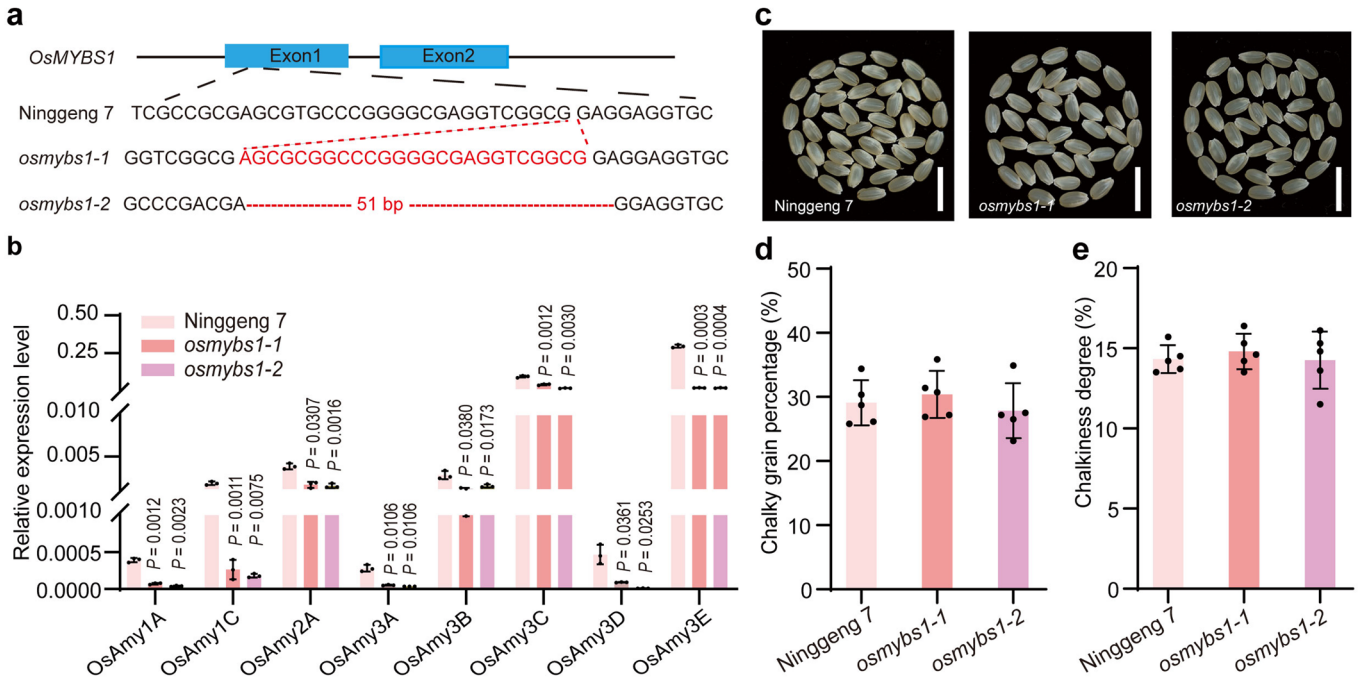

Extended Data Fig. 2 | Phenotypic characterization of the *OsMYBS1* knockout lines. a, Genotyping of the *OsMYBS1* knockout lines. *osmybs1-1* carries a 17-bp insertion, while *osmybs1-2* harbors a 51-bp deletion. **b**, Expression of α-Amylase genes in 12 DAF grains of Ninggeng7 and the *OsMYBS1* knockout lines ($n = 3$ plants). **c**, Mature grains of Ninggeng7 and the *OsMYBS1* knockout lines. Scale bars, 1 cm. **d**,**e**, Chalky grain percentage (**d**) and chalkiness degree (**e**) of mature grains of Ninggeng 7 and the *OsMYBS1* knockout lines ($n = 5$ plants). Values in **b**, **d** and **e** are means ± s.d. Statistical significance in **b**, **d**, and **e** was determined by a two-tailed Student's *t* test.

https://doi.org/10.1038/s41588-025-02429-2

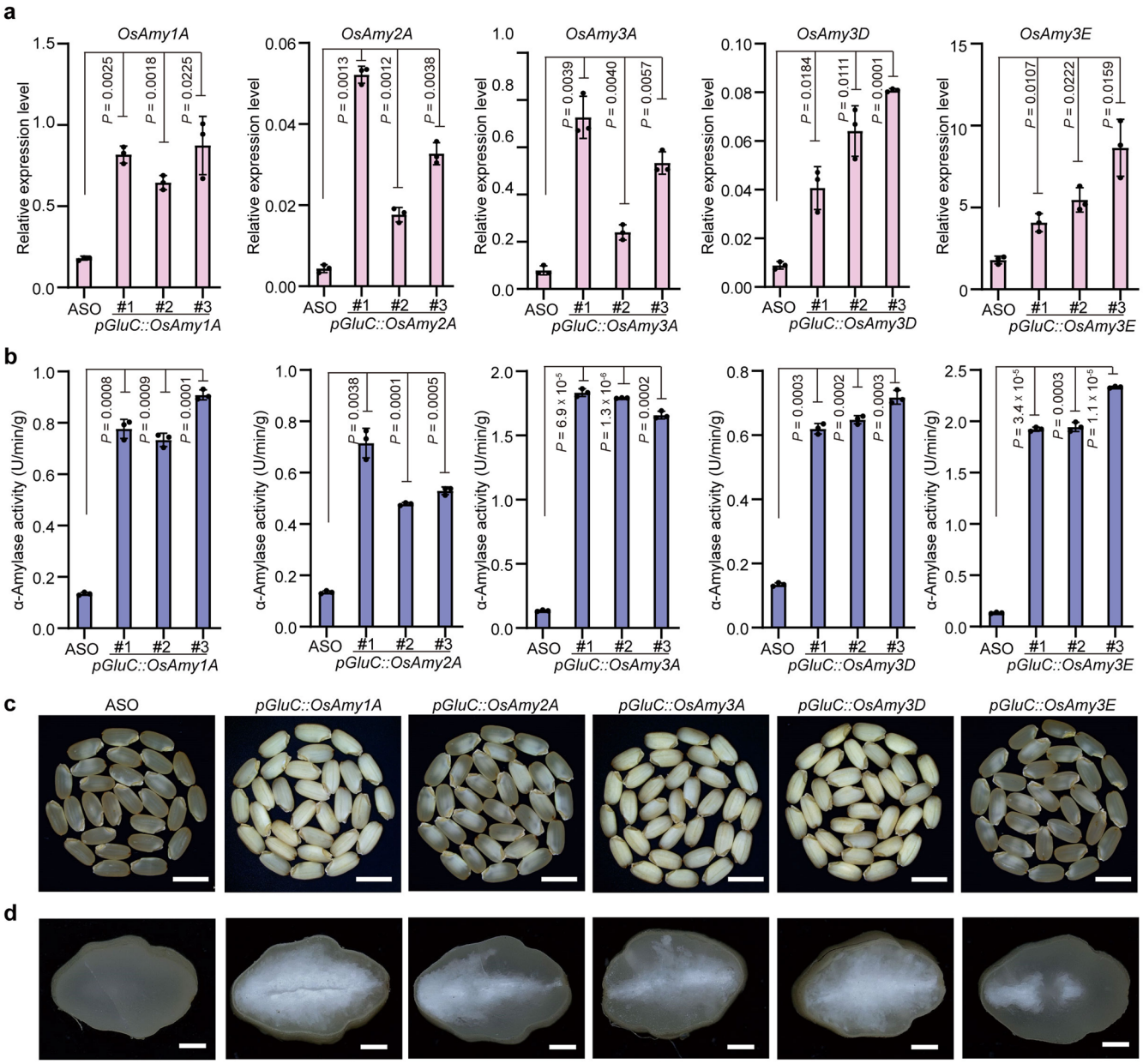

Extended Data Fig. 3 | Phenotypic characterization of *α-amylase* gene overexpression lines. a, Expression levels of α-amylase genes in 15 DAF grains of the overexpression lines ($n = 3$ plants). #1, #2, and #3 represent three independent transgenic lines. **b**, α-amylase activity assay using 15 DAF grains ($n = 3$ plants). **c**,**d**, Mature grains (**c**) and transverse sections (**d**) for α-amylase gene overexpression lines. Scale bars, 5 mm (**c**) and 0.5 mm (**d**). Values in **a**, **b** are means ± s.d. Statistical significance was determined by a two-tailed Student's *t* test.

https://doi.org/10.1038/s41588-025-02429-2

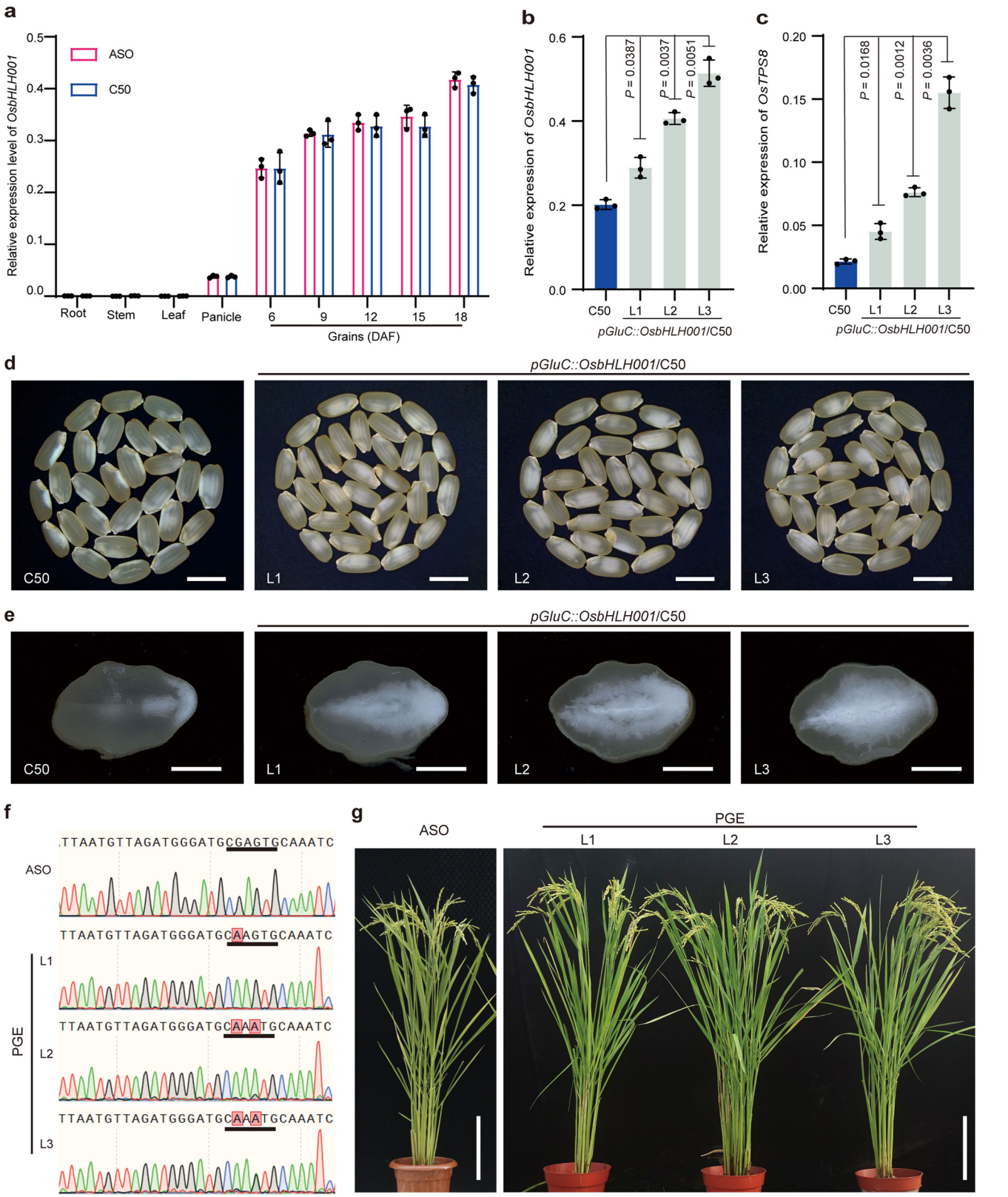

Extended Data Fig. 4 | OsbHLH001 binds to the CAAGTG motif to exaggerate chalkiness. a, Spatiotemporal expression patterns of *OsbHLH001* in ASO and C50 ($n = 3$ plants). **b**,**c**, Expression levels of *OsbHLH001* (**b**) and *OsTPS8* (**c**) in the *pGluC::OsbHLH001* transgenic lines in the C50 background ($n = 3$ plants). L1, L2, and L3 represent three independent transgenic lines. **d**,**e**, Mature grains (**d**) and transverse sections (**e**) of C50 and the *pGluC::OsbHLH001* positive lines. Scale bars, 5 mm (**d**) and 1 mm (**e**). **f**, Genotyping of the targeted base-editing mutations in the *OsTPS8* promoter. L1, L2, and L3 represent three independent PGE lines. **g**, Morphology of ASO and three independent PGE lines at the grain-filling stage. Scale bars, 20 cm. Values in **a**-**c** are means ± s.d. Statistical significance was determined by a two-tailed Student's *t* test.

https://doi.org/10.1038/s41588-025-02429-2

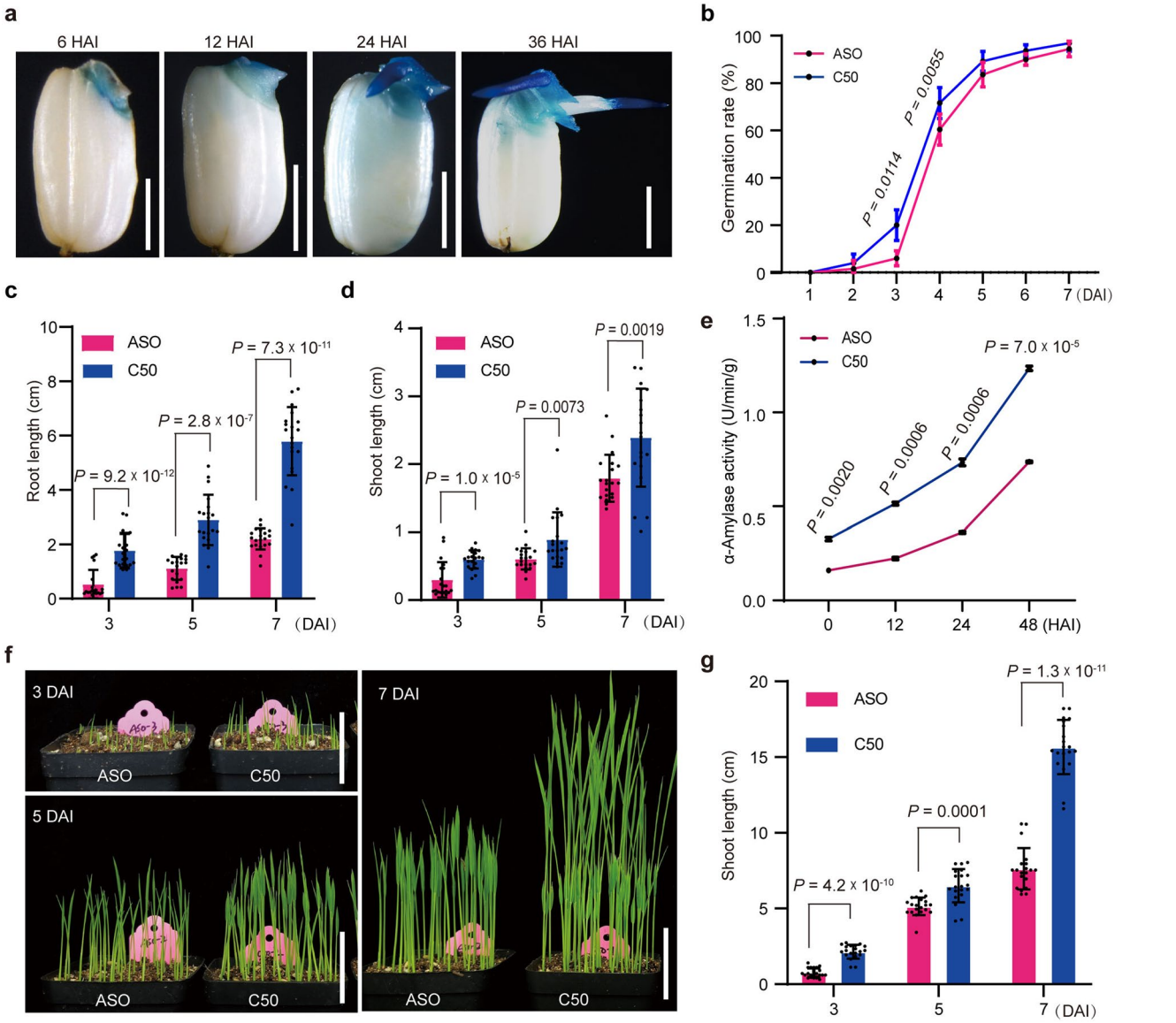

Extended Data Fig. 5 | Phenotypic differences in seed vigour between ASO and C50. a, Histochemical staining for βGUS activity in imbibed seeds. HAI, Hours after imbibition. Scale bars, 5 mm. **b**, Dynamic changes of germination rate between ASO and C50 ($n = 5$ biological replicates). DAI, days after imbibition. **c**,**d**, Root length (**c**) and shoot length (**d**) of ASO and C50 germinated seeds at 3, 5, and 7 DAI ($n = 20$ seeds). **e**, α-amylase activities in seeds at different imbibition stages ($n = 3$ plants). **f**, Early seedling development of ASO and C50 grown in soil. Scale bars, 5 cm. **g**, Shoot length of ASO and C50 seedlings at 3, 5, and 7 DAI grown in soil ($n = 20$ seeds). Values in **b**-**e**, and **g** are means ± s.d. Statistical significance was determined by a two-tailed Student's *t* test.

https://doi.org/10.1038/s41588-025-02429-2

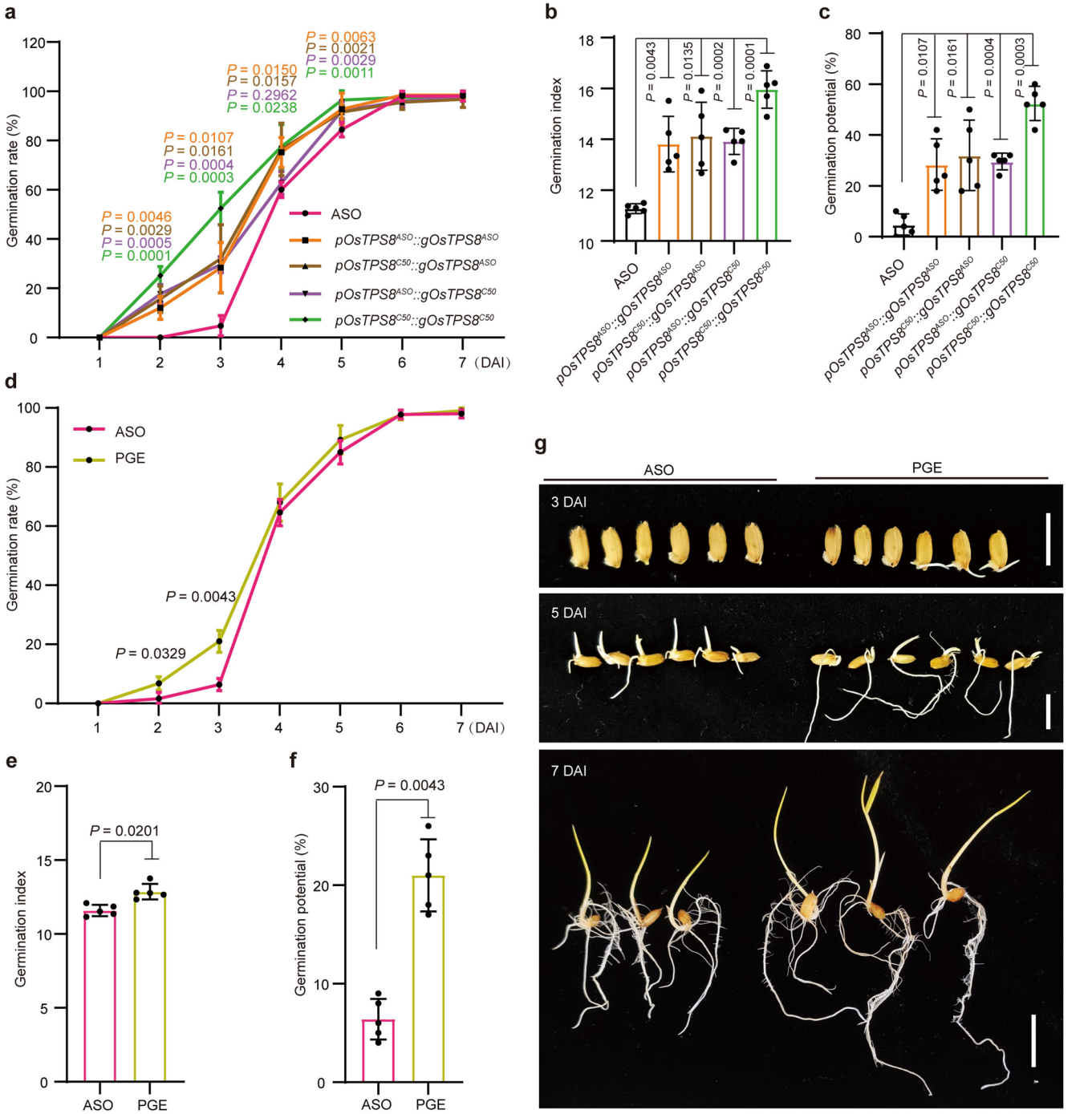

Extended Data Fig. 6 | *OsTPS8* positively regulates seed vigour. a, Dynamic changes in germination rate between ASO and *OsTPS8* transgenic lines ($n = 5$ biological replicates). **b**,**c**, Germination index (**b**) and germination potential (**c**) of ASO and *OsTPS8* transgenic lines ($n = 5$ biological replicates). (**d**) Dynamic changes in germination rate between ASO and the PGE lines ($n = 5$ biological replicates). **e**,**f**, Germination index (**e**) and germination potential (**f**) of ASO and the PGE lines ($n = 5$ biological replicates). **g**, Representative images showing the differences in germination between ASO and the the PGE lines. Scale bars, 2 cm. Values in **a-d**, **e**, and **f** are means ± s.d. Statistical significance was determined by a two-tailed Student's *t* test.

https://doi.org/10.1038/s41588-025-02429-2

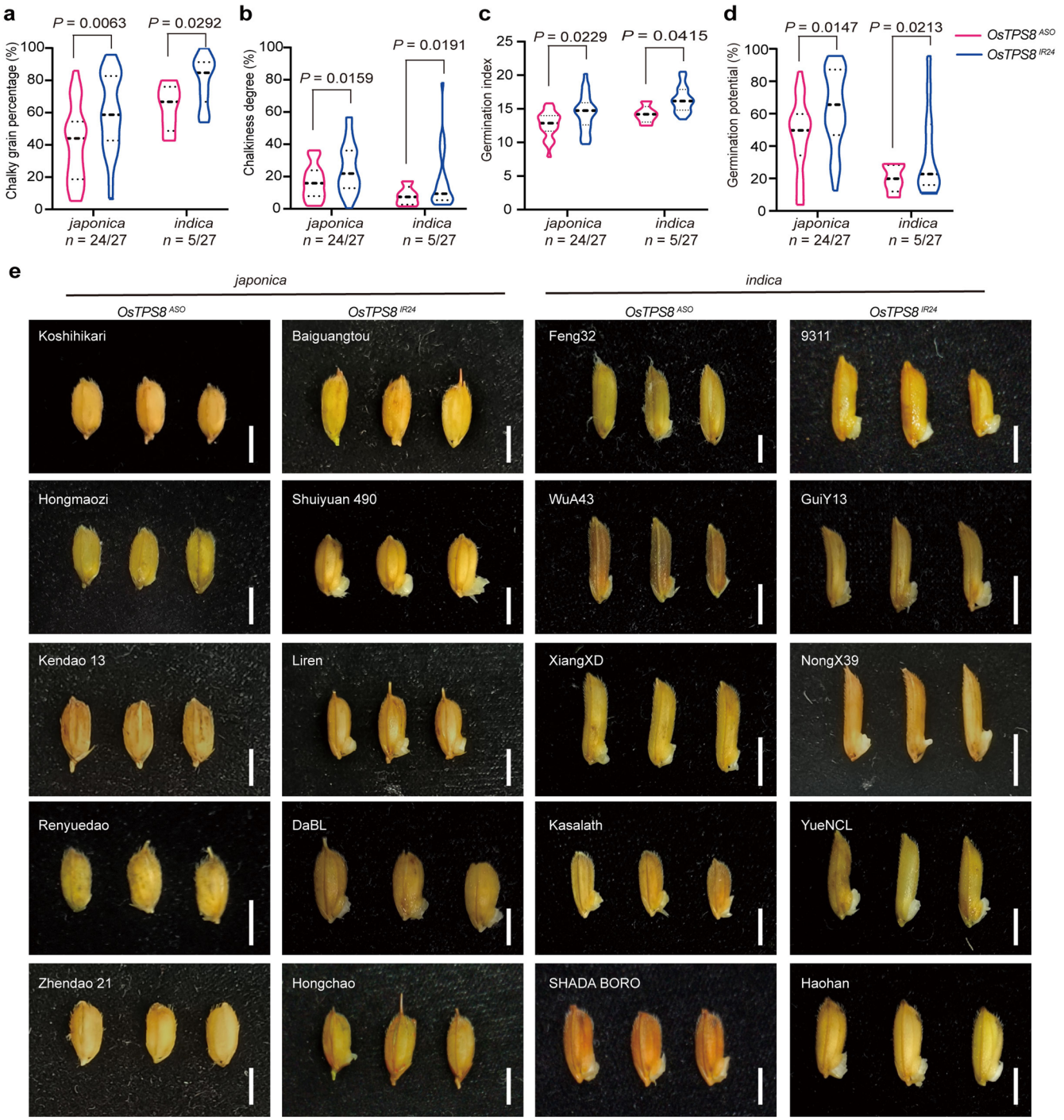

Extended Data Fig. 7 | *OsTPS8* haplotypes are associated with chalkiness and seed vigour. a-d, chalky grain percentage (**a**), chalkiness degree (**b**), germination index (**c**) and germination potential (**d**) in *japonica* and *indica* accessions harboring different *OsTPS8* haplotypes. Sample sizes in (**a-d**) are 24, 27, 5, and 27 independent rice accessions, respectively. The bold dashed line lines, median values; dashed lines, IQRs in violin plots. **e**, Seed germination of rice accessions with $OsTPS8^{ASO}$ and $OsTPS8^{IR24}$ haplotypes at 3 days after imbibition. Scale bars, 1 cm. Values in **a-d** are means ± s.d. Statistical significance was determined by a two-tailed Student's *t* test.

https://doi.org/10.1038/s41588-025-02429-2

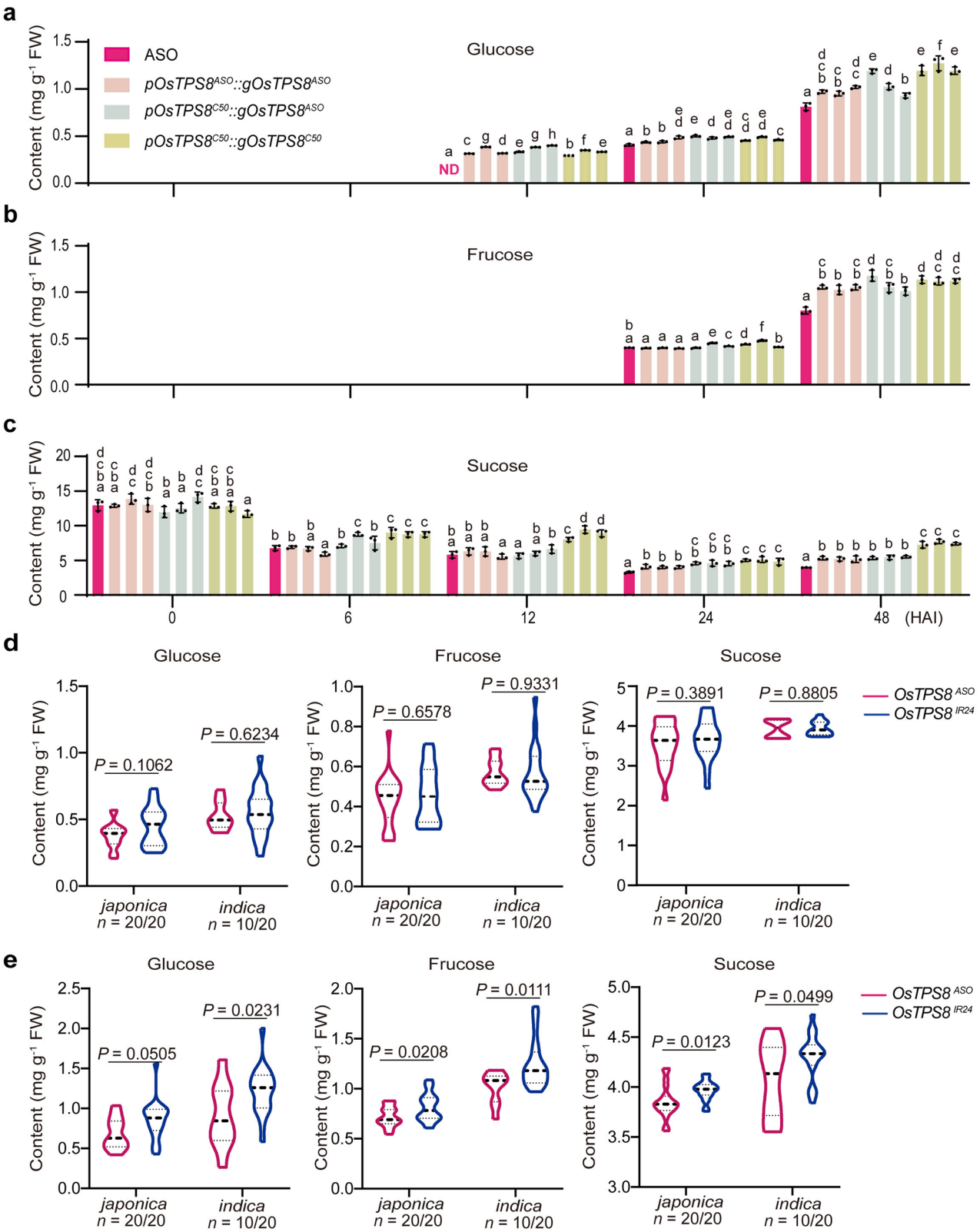

Extended Data Fig. 8 | Determination of soluble sugars in seeds during germination. a-c, Measurements of glucose (**a**), fructose (**b**), and sucrose (**c**) contents in seeds of ASO and the *OsTPS8* transgenic lines at different HAI ($n = 3$ biological replicates). **d**,**e**, Determination of glucose, fructose, and sucrose contents in the brown rice of different rice accessions at 24 HAI (**d**), and 48 HAI (**e**). The bold dashed line lines, median values; dashed lines, IQRs in violin plots. Sample sizes in **d**, **e** are 20, 20, 10, and 20 independent rice accessions, respectively. Values in **a-e** are means ± s.d. Different letters at the top of each column in **a-c** indicate a significant difference at $P < 0.05$ based on one-way ANOVA with Dunnet's multiple comparisons test. Statistical significance in **d**, **e** was determined by a two-tailed Student's *t* test.

https://doi.org/10.1038/s41588-025-02429-2

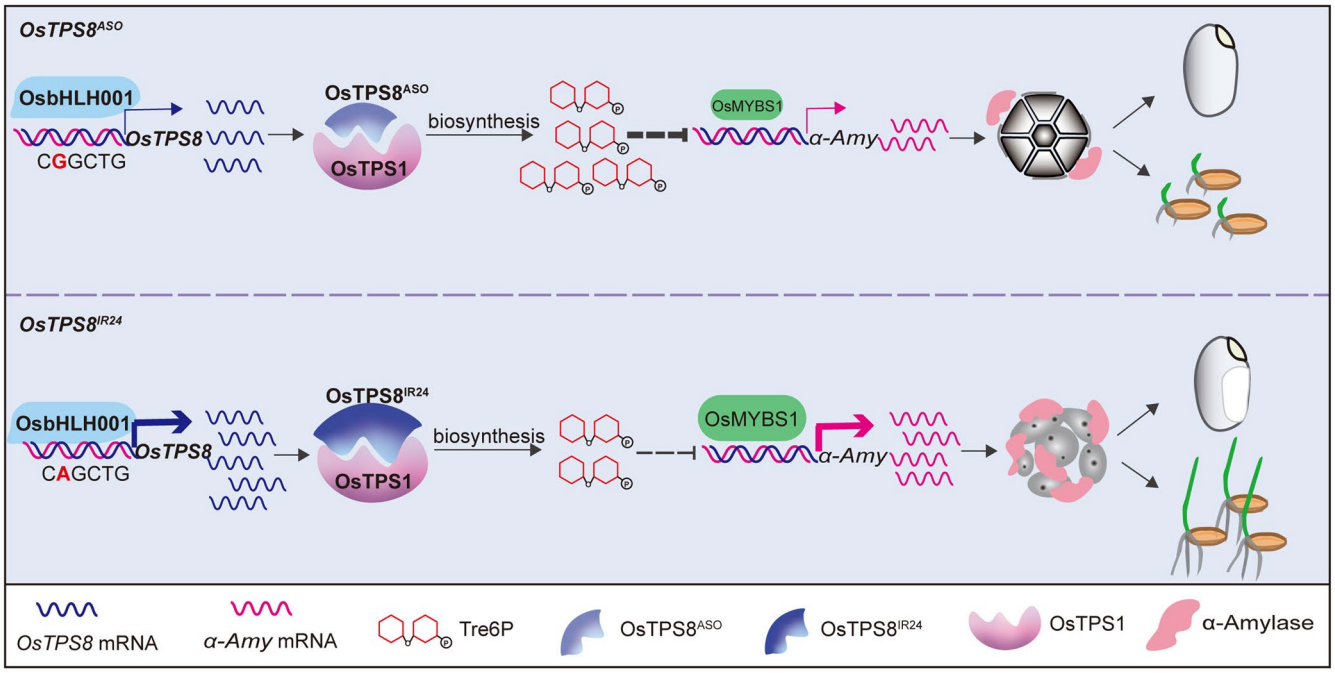

Extended Data Fig. 9 | A working model depicting the function of *OsTPS8* in regulating grain chalkiness and seed vigour. The natural variation -645 A/G in the *OsTPS8* promoter leads to different binding affinities for the transcription factor OsbHLH001, which has a stronger binding ability to the $OsTPS8^{IR24}$ promoter than to $OsTPS8^{ASO}$ to activate *OsTPS8* transcription. OsTPS8 then interacts with OsTPS1 to inhibit Tre6P production in grains. Low Tre6P level decreases its inhibitory effect on the expression of *OsMYBS1* and α-amylase genes, enhancing starch degradation during the late stages of grain development, leading to chalkiness. Concurrently, elevated α-amylase activity promotes seed vigour.

nature portfolio

Corresponding author(s): Jianmin Wan, Yihua Wang, Haiyang Wang

Last updated by author(s): Sep 25, 2025

Reporting Summary

Nature Portfolio wishes to improve the reproducibility of the work that we publish. This form provides structure for consistency and transparency in reporting. For further information on Nature Portfolio policies, see our Editorial Policies and the Editorial Policy Checklist.

Statistics

For all statistical analyses, confirm that the following items are present in the figure legend, table legend, main text, or Methods section.

n/a	Confirmed
☐	☒ The exact sample size (*n*) for each experimental group/condition, given as a discrete number and unit of measurement
☐	☒ A statement on whether measurements were taken from distinct samples or whether the same sample was measured repeatedly
☐	☒ The statistical test(s) used AND whether they are one- or two-sided *Only common tests should be described solely by name; describe more complex techniques in the Methods section.*
☒	☐ A description of all covariates tested
☒	☐ A description of any assumptions or corrections, such as tests of normality and adjustment for multiple comparisons
☐	☒ A full description of the statistical parameters including central tendency (e.g. means) or other basic estimates (e.g. regression coefficient) AND variation (e.g. standard deviation) or associated estimates of uncertainty (e.g. confidence intervals)
☐	☒ For null hypothesis testing, the test statistic (e.g. *F*, *t*, *r*) with confidence intervals, effect sizes, degrees of freedom and *P* value noted *Give P values as exact values whenever suitable.*
☒	☐ For Bayesian analysis, information on the choice of priors and Markov chain Monte Carlo settings
☒	☐ For hierarchical and complex designs, identification of the appropriate level for tests and full reporting of outcomes
☒	☐ Estimates of effect sizes (e.g. Cohen's *d*, Pearson's *r*), indicating how they were calculated

Our web collection on statistics for biologists contains articles on many of the points above.

Software and code

Policy information about availability of computer code

Data collection	Chalkiness degree and chalky grain percentage were measured by a rice appearance quality detector (JMWT12, SATAKE, Tokyo); Microscopy observations were observed with a Hitachi Regulus 8100 scanning electron microscope (Hitachi, Tokyo); Quantitative real-time PCR assays were performed on a Bio-Rad T100TM real-time PCR system (California); Subcellular location were observed with confocal laser scanning microscope (Leica TCS-SP8); Tre6P and enzymatic reaction products were measured with an LC/MS system (ACQUITY UPLC I-Class PLUS coupled with Xevo TQ-S Micro MS/MS, Waters); The firefly LUC and REN activities were measure by a chemiluminescence detector (Promega GloMax20/20). Soluble sugars were determined by HPLC (Waters, H class)
Data analysis	Microsoft Excel 2016; GraphPad Prism v8.0.1 and SPSS v17.0 (one-way ANOVA, Duncan's multiple range test); Single gene association analysis was performed by GWAS-rMVP R package; LDBlockShow v1.40 software was utilized to carry out the pairwise linkage disequilibrium analysis; The geographic distribution was conducted on map using R package ggplot2. Nucleotide diversity (π) and Fst were calculated by VCFtools software (https://vcftools.github.io/).

For manuscripts utilizing custom algorithms or software that are central to the research but not yet described in published literature, software must be made available to editors and reviewers. We strongly encourage code deposition in a community repository (e.g. GitHub). See the Nature Portfolio guidelines for submitting code & software for further information.

Data

Policy information about availability of data

All manuscripts must include a data availability statement. This statement should provide the following information, where applicable:

- Accession codes, unique identifiers, or web links for publicly available datasets
- A description of any restrictions on data availability
- For clinical datasets or third party data, please ensure that the statement adheres to our policy

The data supporting the findings of this study are available in the article and its Supplementary Information files. For the phylogenetic analysis of OsTPS8, genomic sequences of 1453 rice accessions (359 wild accessions and 1094 rice landraces) were obtained from Jing et al. The code and source data for the bioinformatic analyses in this study have been deposited in the Zenodo repository (https://zenodo.org/records/17393751). Source data are provided with this paper.

Research involving human participants, their data, or biological material

Policy information about studies with human participants or human data. See also policy information about sex, gender (identity/presentation), and sexual orientation and race, ethnicity and racism.

Reporting on sex and gender	not involved.
Reporting on race, ethnicity, or other socially relevant groupings	not involved.
Population characteristics	not involved.
Recruitment	not involved.
Ethics oversight	not involved.

Note that full information on the approval of the study protocol must also be provided in the manuscript.

Field-specific reporting

Please select the one below that is the best fit for your research. If you are not sure, read the appropriate sections before making your selection.

☒ Life sciences ☐ Behavioural & social sciences ☐ Ecological, evolutionary & environmental sciences

For a reference copy of the document with all sections, see nature.com/documents/nr-reporting-summary-flat.pdf

Life sciences study design

All studies must disclose on these points even when the disclosure is negative.

Sample size	Sample size are indicated in individual figures and figure legends. To evaluate chalkiness phenotype in the field, at least 5 samples were investigated. For evaluation of agronomic traits, at least 10 samples were investigated. For the expression level quantification of genes, 3 biological replicates were performed for each sample. For subcellular localization analysis, at least 3 biological replicates were observed. For LC-MS/MS analysis, 3 biological repeats were performed. For single gene association analysis, 331 Asian cultivated rice accessions were planted in 2019 and 2020 in Hainan, China. For phylogenetic analysis of OsTPS8, the genomic sequences of 1453 rice accessions were obtained from Jing et al, which consists of 359 wild accessions and 1094 rice landraces.
Data exclusions	No data excluded.
Replication	All experiments in this study were repeated independently at least three times. For RT-qPCR three biologically independent samples were used each time. For subcellular localization, physiological and biochemical experiments, the results representative of three independent experiments.
Randomization	For field experiments, the varieties and transgenic lines were grown in a completely-randomized block design with three replicates. We always randomly selected the samples based on the genotype for experiments.
Blinding	For all experiments, we always performed three or more than three replicates or measurements without human interference, therefore, we did not perform blinding analysis.

Reporting for specific materials, systems and methods

We require information from authors about some types of materials, experimental systems and methods used in many studies. Here, indicate whether each material, system or method listed is relevant to your study. If you are not sure if a list item applies to your research, read the appropriate section before selecting a response.

Materials & experimental systems

n/a	Involved in the study
☐	☒ Antibodies
☒	☐ Eukaryotic cell lines
☒	☐ Palaeontology and archaeology
☒	☐ Animals and other organisms
☒	☐ Clinical data
☒	☐ Dual use research of concern
☐	☒ Plants

Methods

n/a	Involved in the study
☒	☐ ChIP-seq
☒	☐ Flow cytometry
☒	☐ MRI-based neuroimaging

Antibodies

Antibodies used

1. Anti-GFP (Roche, 11814460001, NA, 1:2000);
2. Anti-cFBPase (Agrisera, AS04 043,NA, 1:3000)
3. Anti-Histone H3(Abcam, ab1791, NA,1:5000)
4. Anti-GST (MBL, PM013-7, NA,1:5000)
5.Anti-Flag (Sigma-Aldrich, A8592, NA, 1:5000)
6. Goat Anti-Rabbit (MBL, 458, NA, 1:5000)
7. Goat Anti- Mouse (MBL, 330, NA, 1:5000)
8. Anti-EF-1α, Anti-AGPL2, Anti-AGPS2b, Anti-SSIIa, Anti-GBSSI, Anti-SBEI, and Anti-PHOI were sourced from Abclonal Biotechnology, have been previously characterized in published research. (Wang, Y. et al. GOLGI TRANSPORT 1B regulates protein export from the endoplasmic reticulum in rice endosperm cells. Plant Cell 28, 2850-2865, (2016)) and Cai et, al. (Cai, Y. et al. OsPKpα1 encodes a plastidic pyruvate kinase that affects starch biosynthesis in the rice endosperm. J. Integr. Plant Biol. 60, 1097–1118. (2018)).
9.The Anti-OsTPS8 and Anti-Amylase antibodies were generated by Abclonal Biotechnology using a peptide synthesis strategy.

Validation

1. Anti-GFP validation could be found in the website: https://www.sigmaaldrich.cn/CN/zh/product/roche/11814460001.
2. Anti-cFBPase validation could be found in the website: https://www.agrisera.com/en/artiklar/cfbpase-cytosolic-fructose-16-bisphosphatase-marker-for-cytoplasm.html
3. Anti-Histone H3 validation could be found in the website: https://www.abcam.com/en-us/products/primary-antibodies/histone-h3-antibody-nuclear-marker-and-chip-grade-ab1791
4. Anti-GST validation could be found in the website: https://www.mblbio.com/bio/g/dtl/A/?pcd=PM013-7
5.Anti-Flag validation could be found in the website: https://www.sigmaaldrich.cn/CN/zh/product/sigma/a8592
6. Goat Anti-Rabbit validation could be found in the website: https://www.mbl-chinawide.cn/search012?keyword=458&field=brand-46&order=&limit=100
7. Goat Anti- Mouse validation could be found in the website: https://www.mbl-chinawide.cn/search012?keyword=330&field=class-39&order=&limit=100
8. Anti-EF-1α, Anti-AGPL2, Anti-AGPS2b, Anti-SSIIa, Anti-GBSSI, Anti-SBEI, Anti-PHOI, Anti-OsTPS8 and Anti-Amylase antibodies may be obtained by contacting the corresponding author, J.M.W.

Plants

Seed stocks

All seeds were collected, stored, and supplied by the State Key Laboratory of Crop Genetics & Germplasm Enhancement and Utilization, Jiangsu Collaborative Innovation Center for Modern Crop Production, Nanjing Agricultural University, China.

Novel plant genotypes

We used the CRISPR/Cas9 technology in generating genome-edited plants. For base-editing, a tiled sgRNA designed to target the promoter of OsTPS8. Annealed oligos were inserted into BsaI (New England BioLabs) digested pH-APOBEC1-SpRY vectors. Agrobacterium-based transformation was used to generate the overexpression lines and the genome-edited rice plants.

Authentication

PCR and Sanger sequencing was used to verify the genome edits generated at the designated genomic targets. RT-qPCR are used to verify the expression of the transgenic lines.